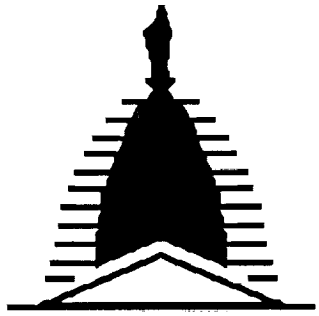

UNIVERSITY of
NOTRE DAME

NASA/USRA UNIVERSITY ADVANCED DESIGN PROGRAM 1988-1989

Final Design Proposal

THE MANTA

An RPV Designed to Investigate
Forces and Moments on a Lifting Surface

Department of Aerospace and Mechanical Engineering
University of Notre Dame
Notre Dame, IN 46556

MANTA

Airborne Data Acquisition System

Designed by:

Kevin Bryan
John Soutar
Peter Witty
Bruno Mediate
Thomas Quast
Dan Combs
Martin Schubert
David Condron
Scott Taylor
Ed Garino
Chris Weppner

1.0 Executive Summary

The remotely piloted vehicle documented in this report was designed to collect aerodynamic data on airfoil or wing planform test sections at low Reynolds numbers. The aircraft test section is located forward of the aircraft to insure an undisturbed air flow over the test section. Due to its "manta ray" appearance, this craft has been dubbed MANTA by the design team. The aircraft has a 19.4 ft wingspan, an aspect ratio of 13 and a fuselage length of 11.8 ft. The aircraft is fitted with twin 3 hp gas engines mounted on either wing. Data will be taken using a force-balance system patterned after a NASA design and then radioed to a ground receiver. The MANTA incorporates an automated control system which will control the craft during the data acquisition phase of the flight.

1.1 Design Goals

MANTA was conceived in response to an RFP originating from the University of Notre Dame Aerospace Department and received in January 1989. The points of contact for the RFP are Dr. S. Batill and Dr. P.Dunn. The goal of the MANTA vehicle is to collect actual flight load data for any type of rectangular or tapered airfoil section including vertical and horizontal stabilizers. The variation in test section angle will be from -20 to 40 degrees with the Reynolds number varying in a range from 40,000 to 1,000,000. The MANTA must be able to take off in a 150 ft radius circle and have a 50 ft object clearance. All ground operations must be handled by no more than two persons and the system must be portable in a pickup truck.

TABLE OF CONTENTS

1.2 Design Constraints

The MANTA aircraft is designed for flight under clear weather conditions only. It is operated under line-of-sight conditions due specifically to the nature of the remote control system and the two man limitation of the ground operations team. The amount of wind in which the MANTA can safely operate and the effect of wind gusts on the aircraft still needs to be determined. The MANTA is designed to take off using a conventional landing gear arrangement. Two wheels are located on either side of the fuselage beneath the wing, and the third wheel is a steerable tail wheel located just beneath the vertical stabilizer.

A study of the priorities given to design criterion has yielded the following prioritization of mission goals:

1. Flexibility of test conditons: alpha, Re, specimen type
2. Accurate, usable data collection
3. Good durability
4. Wide operating range
5. Efficient cruise performance
6. Marketability
7. Low aircraft weight
8. Cost
9. Takeoff and landing performance
10. Ease of use
11. Ease in manufacturing

Based on these criteria, many designs were proposed and evaluated. The final concept selected places the test section forward of the aircraft fuselage and wing. The test section is supported by two booms which are

located on either side of the fuselage with a constant separation distance of 2 ft. This allows a maximum test section span of 2 ft. Twin 3 hp engines are mounted on either wing 4 ft from the fuselage centerline. The empannage is located 7 ft from the aircraft center of gravity. The vertical tail has been sized to provide directional stability and to allow a safe landing under one engine out conditions. The horizontal tail is sized to insure longitudinal stability throughout the Reynolds number range and the test specimen angle of attack range. The final specifications of the MANTA vehicle can be seen in Figures 1.1 through 1.3 and also in Table 1.1.

1.3 Problem Technology Areas

One of the most difficult tasks involved the proper sizing and movement of the horizontal stabilizer. Large amounts of lift will be generated by the test section at the high angles of attack before the specimen stalls. This large amount of lift will produce a large moment which must be overcome by the horizontal tail. At present the horizontal tail is sized so as to allow full test section angle of attack range. However, this will sometimes dictate that the aircraft itself must actually fly at a negative angle of attack to achieve steady level flight. Data collection while the aircraft is in a steep turn or dive is being investigated to determine feasibility and possible benefits over straight and level flight data collection.

Another area of difficulty encountered is the syncronization of the two gas engines. To avoid yaw moments created by engines operating at different rpm's, the two engines are connected to one servo. The engine rpm's must be matched during ground testing to insure compatibility during flight operations.

A final area of difficulty is determining the lift effects of the fuselage. In order to support the booms, the fuselage is wide-bodied and

Figure 1.2

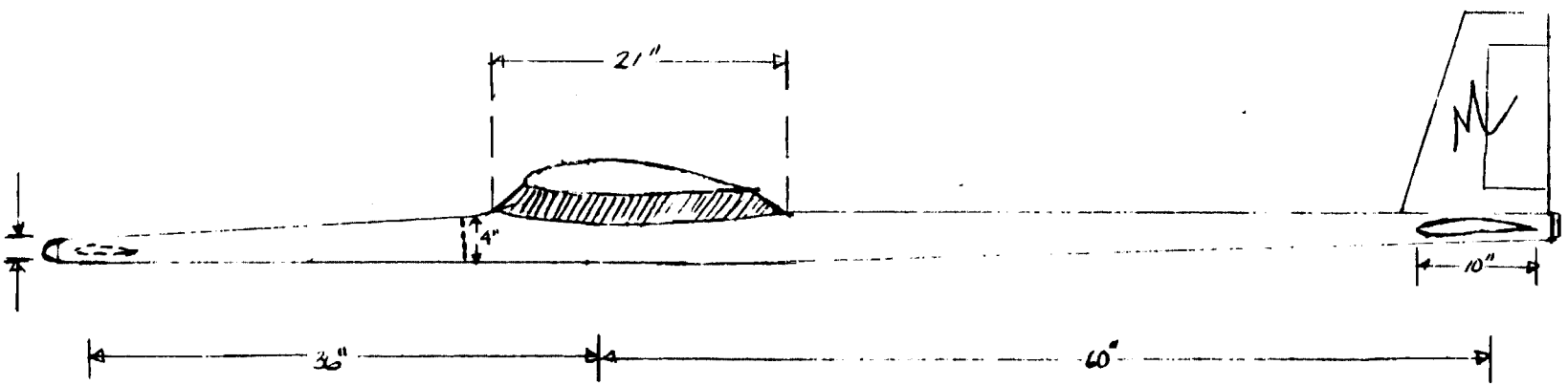

SCALE
1:16

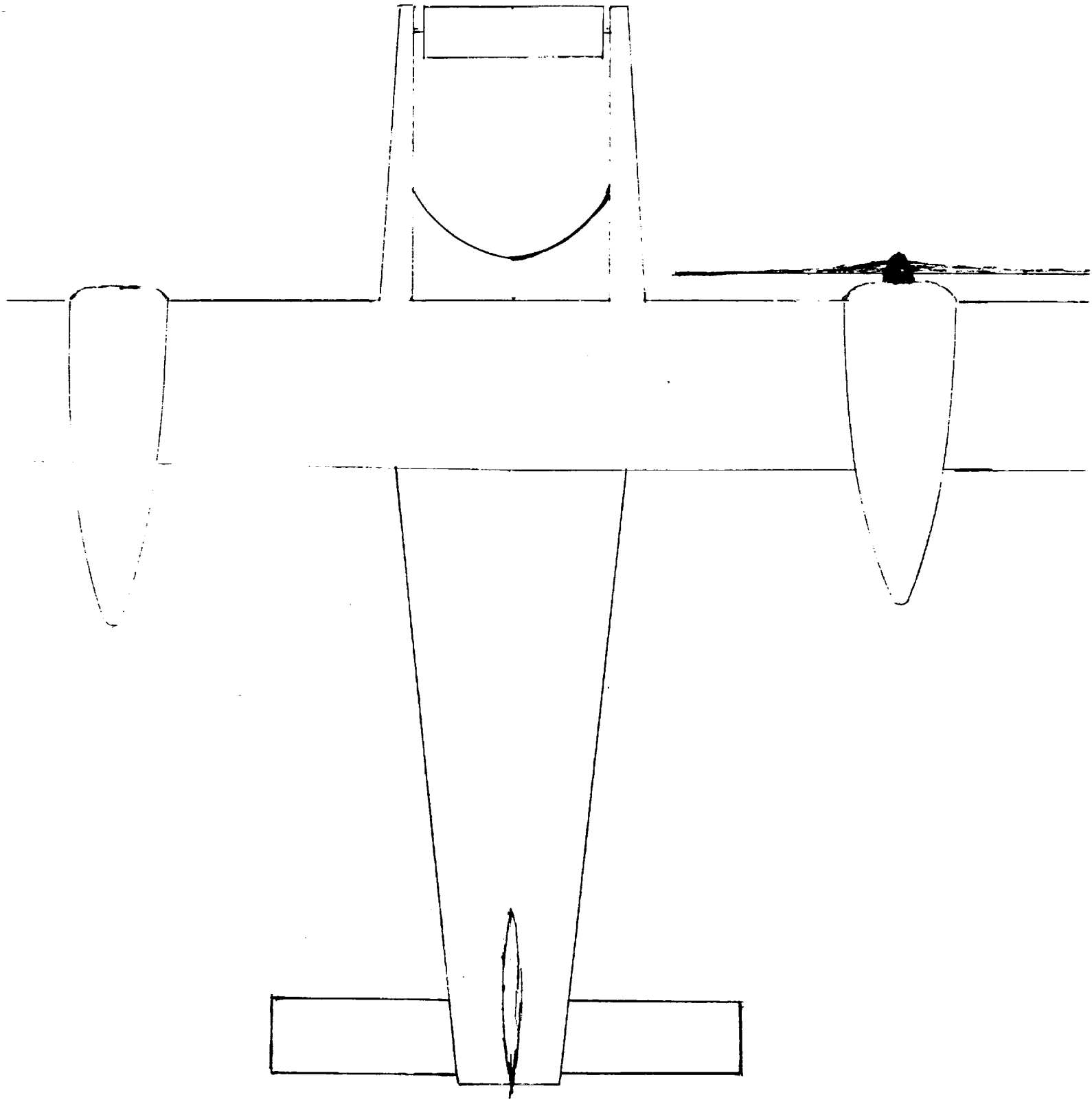

Figure 1.1

will therefore create lift in a manner similar to that of a flat plate. The actual effect must be studied in order to insure that desirable stability and handling characteristics are obtained during flight.

Final Aircraft Specifications

	Nomenclature	Value
Wing Area	Sw	29 [ft^2]
Wing Span	b	19.41 [ft]
Aspect Ratio	AR	13
Weight	W	30 [lb]
Vertical Tail Area	Sv	3.4 [ft^2]
Horizontal Tail Area	Sh	2.7 [ft^2]
Engine Size	sbhp	3 bhp/engine
Propeller Diameter	D	2.0 [ft]
Fuselage Length	lf	10.83 [ft]

Table 1.1

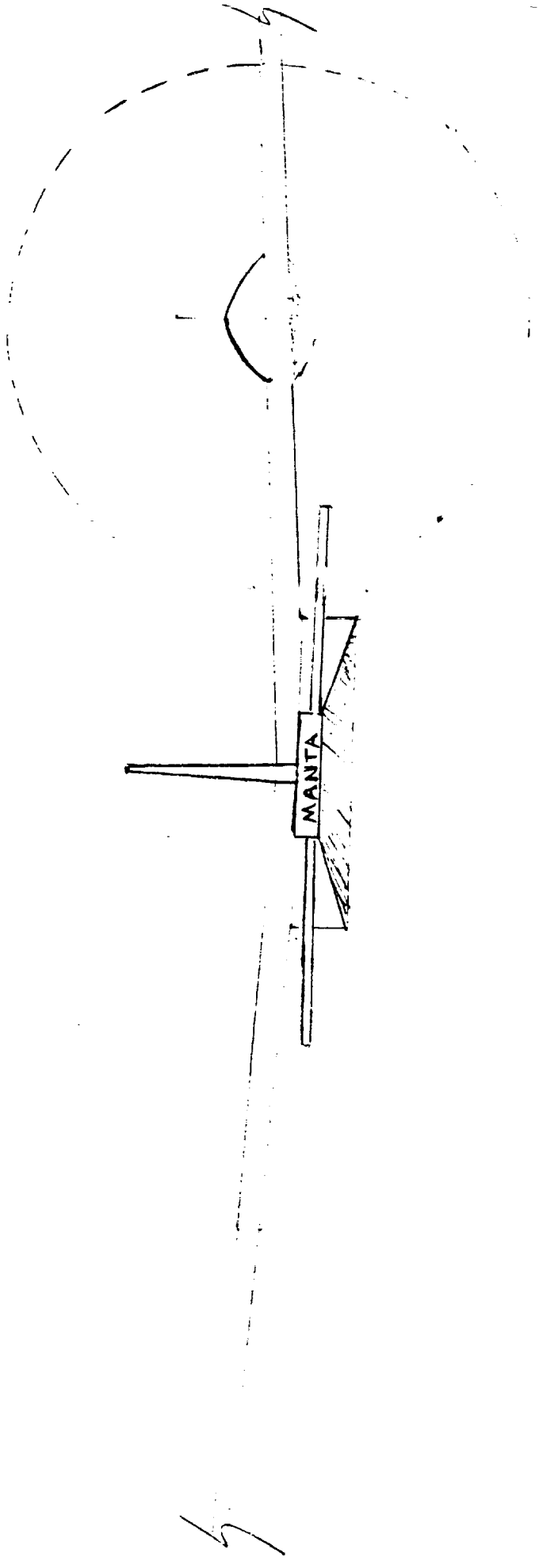

Figure 1.3

2.0 MISSION AND CONCEPT SELECTION

2.1 MISSION REQUIREMENTS

Highlights of the Request for Proposal that this design attempts to meet are given in Table 2.1. The overall goal of this design effort was to investigate the advantages of using remotely piloted vehicles (RPVs) for in-flight data collection, especially for low Reynolds numbers, and to exploit these advantages.

Table 2.1 RFP Highlights.

Objectives:

1. Build an RPV to
    a. collect data with a variety of airfoils
    b. collect at alphas from -20 to 40 deg and Re #s from $4x10^4$ to $1x10^6$
    c. use rectangular and tapered test specimens
    d. be fully instrumented to obtain accurate data
2. Make the system modern, lightweight, reliable, and safe
3. Develop a Demonstrator for this technology

Requirements and Constraints:

1. Line of Sight operation
2. 150ft radius takeoff and landing; turnaround in 15 min.
3. Clear weather capability, with slight gusts and freestream gradient given
4. Instrumentation must be included in design
5. Ground handling by two people
6. System must be portable
7. Noise must be considered

The mission can be divided into two general categories, which are data acquisition and performance. The goals of the mission are contained in the data acquisition category, with the constraints on the vehicle included in the performance category.

There are several data acquisition goals listed in the RFP. The first set requires that flight load data from the RPV be collected and available, either in real time by being telemetered to the ground, or by being recorded and stored on-board for later retrieval. This load data should be available for wing and horizontal and vertical stabilizers. In particular, the capability to study the effects of different airfoil sections on these flight loads is desired. The operating ranges for these tests are wide, to say the least. A Reynolds number range from $4x10^4$ to $1x10^6$ is desired, encompassing the entire low Reynolds range. The desired angle of attack range for the test sections is from -20 deg to 40 deg. In addition, the ability to study both rectangular and tapered sections is required.

In order to make the flight load data as accurate as possible with an RPV testing environment, the corresponding freestream data must be taken by the vehicle. This freestream data includes airspeed, angle of attack, and control surface position.

While performing the mission, the vehicle must meet certain constraints as detailed in the RFP. The maximum takeoff length is 150 ft, with a 50 ft object clearance. The system must have a turnaround time of 15 minutes. Structurally, the vehicle must be sound enough to withstand loads induced by gusts of up to 10 fps above freestream velocity. The vehicle must be able to perform its mission in wind speeds of up to 20 mph, with the exact altitude gradient information as given in the RFP. All mission objectives must be accomplished within the line of sight of the operator. In addition, all ground handling must be capable of being accomplished by two persons, and the vehicle must be of a size such that it could be easily transported in a pickup truck. Finally, noise produced by the vehicle must be taken into consideration.

2.2 MISSION PRIORITIES

Before beginning our individual preliminary concepts, Group C assembled a list of priorities that our designs should try to meet. This list is given in Table 2.2.

Table 2.2 Group C Mission Priorities.

flexibility
data collection
durability
operating ranges
cruise performance
saleability
weight
cost
t/o-landing performance
ease of use
manufacturability

It was decided that the most important mission priority would be mission flexibility. A vehicle that has a wide range of applications will be more appealing and useful than one designed for a single objective. The second priority was quality and quantity of data acquisition. The vehicle is a research tool, and any tool is more valuable if it does more and does it better. Sacrificing quality of data acquisition for, say, gaining 10 MPH of speed is unacceptable. Next on the list is durability. This could be seen as related to data acquisition, as a vehicle cannot collect data if it is inoperative, and cannot collect

good data if it is handicapped in some way by damage. Also, a durable plane will cost less to the researcher in the long run. With these top three priorities settled upon, most of the other priorities in the list fall into place, ie. a versatile, durable, useful plane will be saleable to most concerns. Where there are conflicts with other priorities, ie. cost, it was decided that the advantages gained from meeting one of the three top priorities outweigh the disadvantages from meeting the lesser one.

2.3 INDIVIDUAL CONCEPTS

A wide range of concepts were produced by the eleven individuals in Group C. Each has its unique advantages and disadvantages, but all fall into four rough categories: 1) false wing test specimens, 2) canard/front mounted test specimens, 3) drone aircraft specimen, and 4) wing mounted test specimens. A brief overview of all eleven designs can be found in table 3.

Table 2.3. Overview of Individual Concepts.

#	Distinguishing Characteristics	Advantages	Disadvantages
1	canard,front ts, rear 3d ts	no interf,3d at rear ts	front ts 2d, rear ts interf, canards not proven
2	canard,front ts	3d tests possible	ts interf,canards not proven
3	canard,canard-mount ts, 2d and 3d ts	cleaner flow w/plates,3d	instab at stall,canards not proven
4	canard,drop takeoff	no interf	canards not proven,2d only
5	dorsal-mount horiz ts	small moments	ts interf, 2d only
6	dorsal-mount horiz ts	small moments, 3d poss	ts interf
7	dorsal-mount horiz ts	small moments, 3d poss	ts interf
8	dorsal-mount vert ts	small moments, 3d poss	ts interf, lat stability
9	wingtip ts	cleaner flow w/plates,3d	instab at stall,roll control
10	wingtip ts,canard	cleaner flow w/plates,3d	instab at stall,canards not proven
11	mother/drone, interchang. wings/surfs	no interf,versatile, interf efx tests possible	stab/control,ts control

note: some concepts had names: 2-"Championship 8",9-"Devildog",4-"N88"

In the false wing concepts, a test specimen (ts) was mounted on the dorsal side of the fuselage in either a vertical or horizontal fashion. This specimen would be placed close to the center of gravity (cg) so that the moment produced when the specimen is deflected would be small. Figure 2.1 gives two examples of false wing concepts. These concepts share several advantages. With the moment arm due to the ts being so small, over-sized control surfaces are not needed. With the vertical-mounted and most of the horizontal-mounted designs, three dimensional testing is possible. The vertical-mounted ts has the added advantage of having a fuselage on one end of the

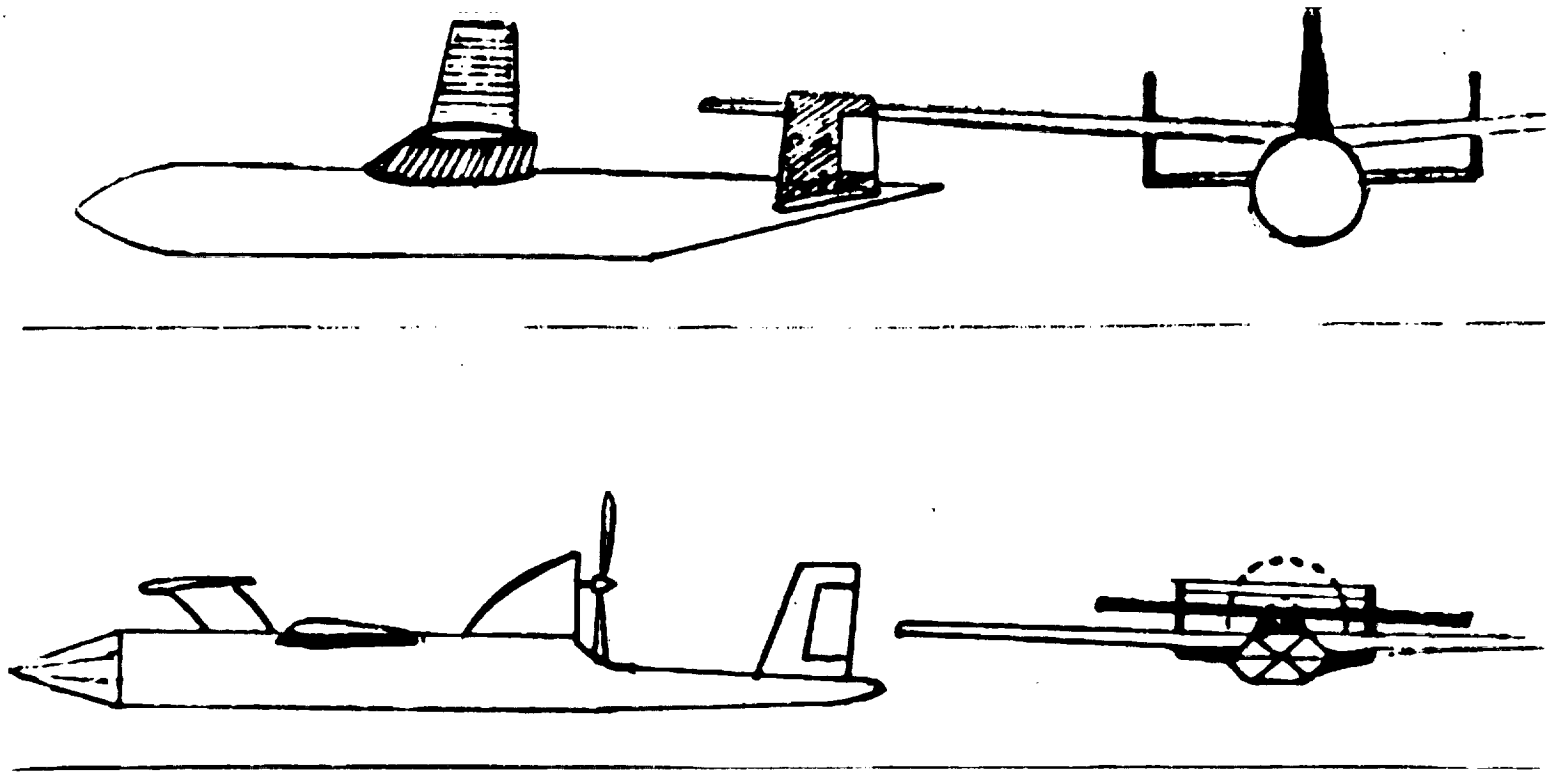

Figure 2.1. Typical False Wing Concepts

specimen, thereby duplicating the wing-fuselage interference effects found in practice, eliminating the need to guess these effects by factoring them in with an empirical method.

The false wing method also has its disadvantages. The greatest of these is aerodynamic interference from the wing and fuselage. With both vertically- and horizontally-mounted models, the fuselage produces a great deal of interference. However, for the vertical specimen, the interference is in a manner that a wing made from the airfoil section would see anyway if it was mounted on the fuselage in a real plane (this was an advantage noted before). With the horizontal, the fuselage induced flow is not in such a beneficial attitude. Any advantages gained by attempts to reduce

interference by moving the ts farther above the fuselage are negated by the deleterious effects of increasing the moment arm to the specimen. With either vertical- or horizontal-mounted specimens, however, a potentially significant amount of interference is caused by the circulation around the wing. This interference reduces the validity of any data acquired using these methods.

The next group of concepts are the canard/front ts concepts. These all had twin frontal booms in between which the ts was mounted. Figure 2.2 shows a typical concepts of this type. In these concepts, instrumentation was mounted in the booms in an attempt to keep the cg near, if not in front of, the aerodynamic center (ac) of the vehicle.

With front-mounted test specimens, there is one extremely important advantage: the lack of aerodynamic interference found. The flow over a front mounted ts should be near-perfect in a well-built plane. This allows the vehicle to meet its goal of quality data acquisition quite nicely.

This one great advantage has its costs. First, the moment arm to the specimen is

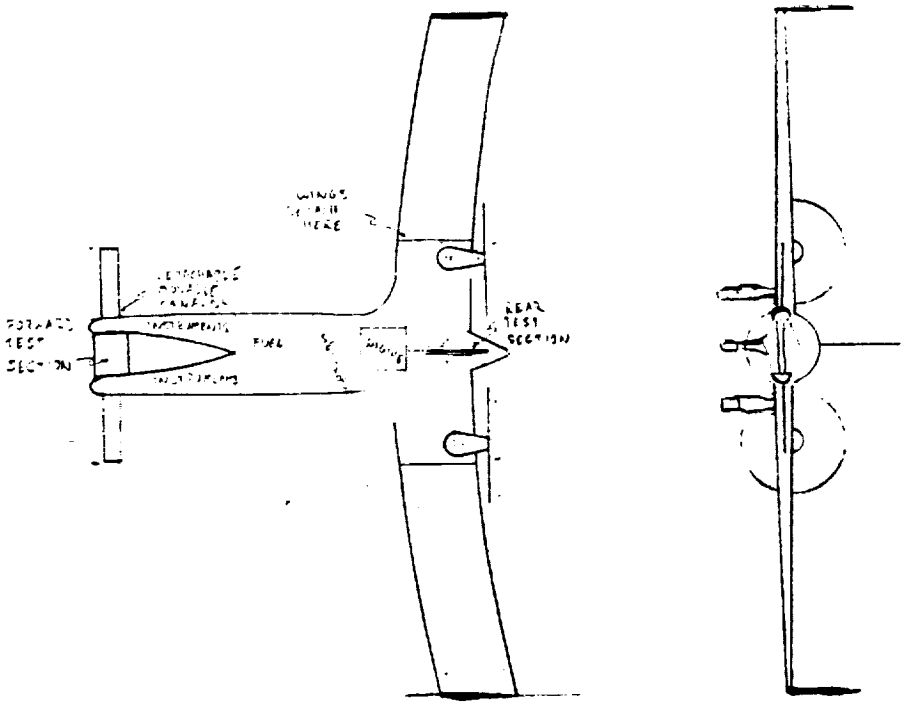

Figure 2. 2 Typical Front Mounted Test Specimen Concepts

greater than that of a dorsally-mounted ts. This necessitates greater control power needed to keep the vehicle in trim, in turn causing reduction in performance, and possibly versatility. Another disadvantage is that only two dimensional effects can be tested with a horizontally-mounted ts. It might be possible to test 3-d effects with a vertical ts mounted on a platform in between the booms, however, as in concept 2, the "Championship 8". This might prove to be too destabilizing in a lateral manner. One final disadvantage of this type of concept is that canard configurations are not proven in RPVs. Very few specimens exist of such craft, and questions remain as to the inherent stability of such craft, even if "the numbers" say they will fly.

Another family of concepts were the wing-mounted test specimens. These include both in-wing and tip-mounted, as can be seen in Figure 2.3. In-wing specimens have endplates on both ends to prevent interference, and are integrated into the wings, one on each side for stability. Tip-mounted specimens are used for 3-d testing, and have one endplate on the inboard end.

There are some benefits to these types of specimens. With big enough endplates, interference can theoretically be reduced. The lift and drag produced by the specimens are nowhere near as destabilizing to the vehicle as with other types, assuming the section is not stalled.

It is when the wing-mounted specimens stall, however, that a problem with them arises. Since stall is a somewhat arbitrary phenomenon, both specimens cannot be expected to stall simultaneously. The flightworthiness of the vehicle is thus severely compromised at this point, as suddenly one section is producing nothing but drag

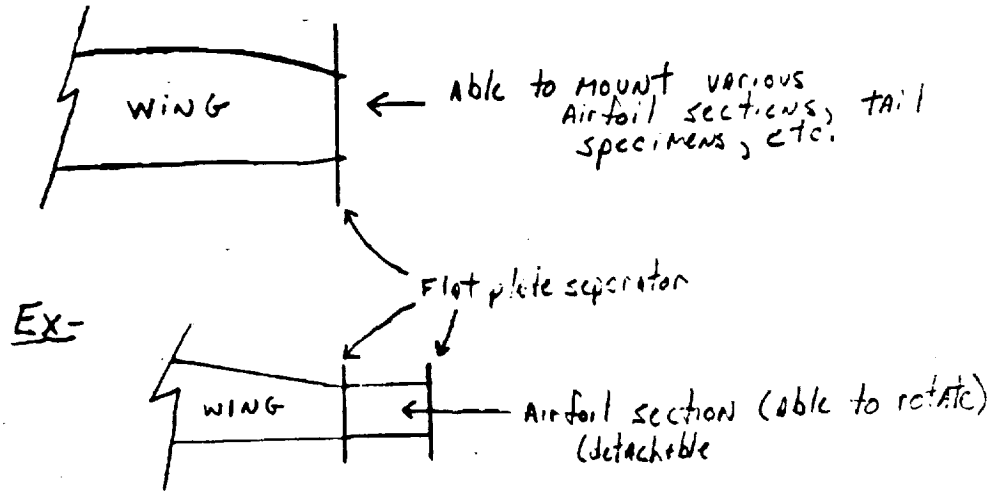

Figure 2.3. Typical Wing Mounted Test Specimen Concepts

while the other is producing near maximum lift.

The final concept was a novel one. It proposed attaching a small, light, drone aircraft to a mothership via a telescopic support. The drone would have movable wings and tail surfaces, but all instrumentation, propulsion, and other systems would be contained in the mothership. A drawing of the concept can be found in Figure 2.4.

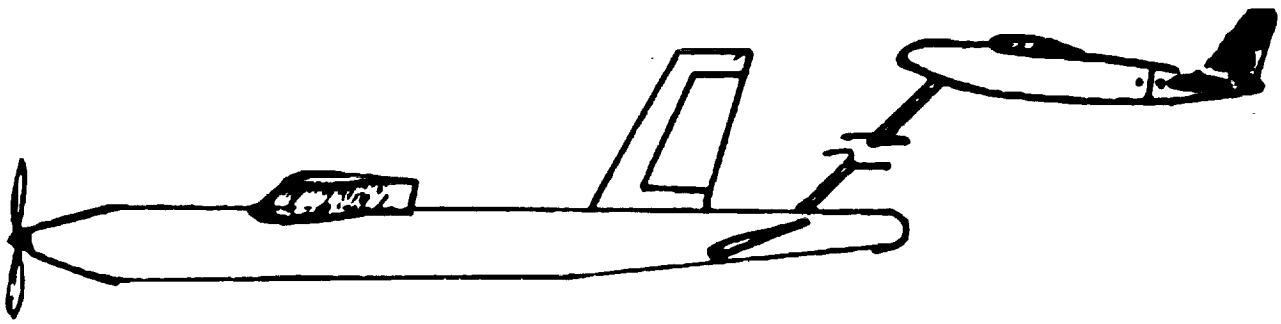

Figure 4. Mothership Drone Concept

This interesting design has several advantages unique among all proposals. First would be an almost complete lack of interference from the mothership. All interference effect on the drone's specimens would be from the drone itself. This would be advantageous, as it was required in the request for proposal to study fuselage-wing interference on RPVs. Thus, not an airfoil section, or even a wing, is tested, but an entire wing-fuselage-empennage assembly. Furthermore, a large number of component combinations can be tested, providing great versatility for this concept.

Unfortunately, there are some serious drawbacks to this concept. They are stability and control and ts control. In order to evacuate itself from the mothership's interference realm, the mothership must be telescoped a considerable distance from the ship. This leads to a huge moment arm from the drone's ac to the mothership's cg. It would dictate enormous control power on the part of the mothership. One could argue that this problem could be overcome by using a very large mothership which would not find the destabilizing moments so severe. However, the constraint on the design is that the system be small enough to be easily portable. In addition, a larger mothership would be inherently more expensive and difficult to produce. Regardless of the mothership's size, there is a problem that would still be difficult to solve easily or cheaply. That is building a telescopic boom thin enough to not produce an unacceptable flow disturbance, and yet long enough to separate the two ships. The flutter that would surely be present during testing could seriously compromise data integrity.

2.4 DECISIONS LEADING TO FINAL PROPOSAL

First, let it be mentioned that the drone concept is worth looking into for this mission, due to its many inherent advantages. However, due to our time and monetary constraints, as well as the unproven ability of the concept to collect decent data, it was decided not to pursue the drone concept.

The wing and wingtip mounted concepts were also passed over, due to their stability concerns. It was decided that these disadvantages outweighed the somewhat clean airflow they provided. Also after further investigation, it was found that the separation plates would have to be extremely large to eliminate interference satisfactorily, to a point where they too would contribute to the interference.

The dorsally-mounted ts concepts were not as easily discarded. While not providing the best data, they were however easily produced due to their conventional design. Placement of the ts so near the cg necessitated only a slight increase in control power over what would be needed for the vehicle without ts. Calculations in the design of such a craft would be straightforward, as would be its manufacture.

In the end though, the integrity of data produced provided the impetus for choosing the front mounted ts. This was with the compromise, though, of choosing a conventional empennage instead of canards. This reduced the "experimental" quality of the vehicle somewhat and better ensured its flightworthiness. The extremely clean airflow resulting from frontal placement of the ts was seen as an advantage that outweighed the concept's disadvantages enough to select it as the basis of our design.

3.0 MANTA MISSION PROFILE

The primary purpose of the MANTA flight vehicle is to collect reliable data over a specified test range. For this reason, the selection of the mission profile needs to reflect that priority. The selection of the MANTA's mission profile also depends upon structural considerations, range and endurance characteristics of the aircraft, and cost considerations. The mission profile of the MANTA can be broken up into three major parts labelled as pre-flight checks and takeoff, in-flight data acquisition, and recovery.

The MANTA will begin its flight mission in the hands of a ground flight controller located at a ground home station near the runway. The ground controller will ensure that the vehicle has the necessary fuel load and that the flight data acquisition system is in working order. Once the ground controller completes his pre-flight checks, the MANTA's twin propeller engines will start, and the flight vehicle will prepare for takeoff. The controller will then power up the engines, taxi the plane down the runway, and take the plane off. The plane will fly in a straight line until it reaches a height of 50 feet and then the controller will maneuver the plane in an upwardly sprialling circle to its predetermined test altitude, approximately 200 feet off of the ground.

Once the MANTA reaches its predetermined test altitude, an automated control system, previously programmed on the ground, will take over flight control of the plane and begin to maneuver the flight vehicle in the data acquisition portion of the flight. In order

to maximize the efficiency of data collection for the MANTA, different shaped flight paths were studied. Specifically, oval, triangular, square, pentagonal, hexagonal, and octagonal flight paths were studied. Each of these flight paths consists of straight line data collection legs connected by constant velocity turns. The use of constant velocity turns ensures constant Reynolds number conditions throughout an entire test.

Three factors contribute directly to the choice of a load factor. First, studies showed that for a specific test velocity, as the load factor of a given constant velocity turn increased, the radius of turn decreased (Figure 3.1). This means that the total perimeter of a flight will decrease as the load factor increases, thus increasing the efficiency of the mission. Second, Figure 3.2 shows that as the load factor increases, the data acquisition time decreases. However, it also shows no significant change between load factors of 1.5 and 3.0. Third, the structures group states that the plane could handle any load factor up to 3.0, having varied the load factor between 1.1 and 3.0. The results of these studies warrant the decision to use a load factor of 1.5. This decision represents a tradeoff between a structural factor of safety and an efficient perimeter for data collection.

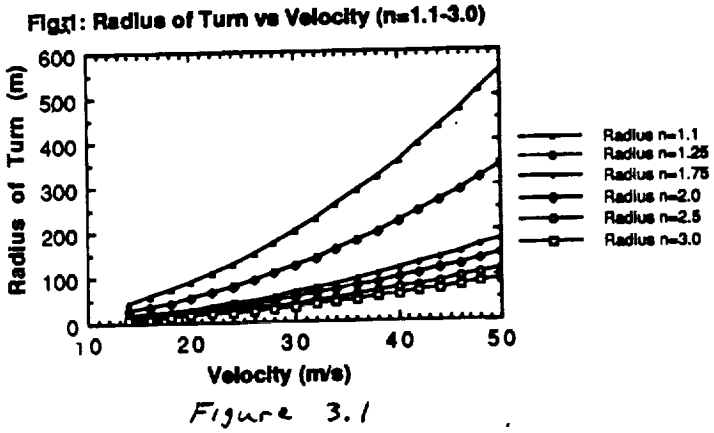

Figure 3.1

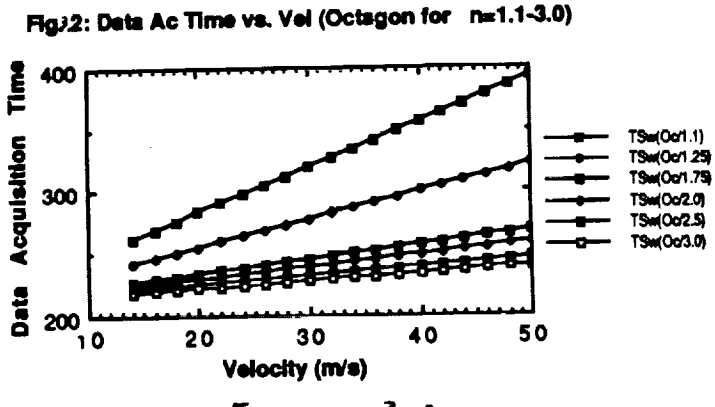

Figure 3.2

The decision of an actual flight path during the data acquisition phase of the mission represents the hardest choice to make. In the end, the flight path needs to satisfy the following requirements. First, the flight path must enable the MANTA to collect the entire amount of data in the least possible number of flight runs. Secondly, each straight line data collection leg of the flight path consists of ten seconds. The first five seconds of the leg enable the control system of the plane to return to steady level flight coming out of a constant velocity turn. The second five seconds are required for actual data collection. Thirdly, a mission constraint requires the use of only 70% of the alotted fuel during the data acquisition phase.

Figure 3.3 shows that the perimeter required to make an entire data sweep decreases as the number of sides of the flight path increases. (i.e. - The octagonal flight path needs less perimeter than the triangular perimter). Studies also show that the time necessary to make an entire data sweep decreases as the number of sides of the flight path increases (Figure 3.4). For these two reasons the initial decision was made to choose the octagonal flight path. Further studies which took into consideration the imposed fuel constraint again led credence to the decision of choosing the octagonal flight path. Figure 3.5 showed that once range and endurance considerations are taken into account the vehicle needs to make only two flight runs to complete the entire data sweep (versus 3 for every other shape).

3.3

Fig. 3: Perimeter vs Velocity (Diff shapes)

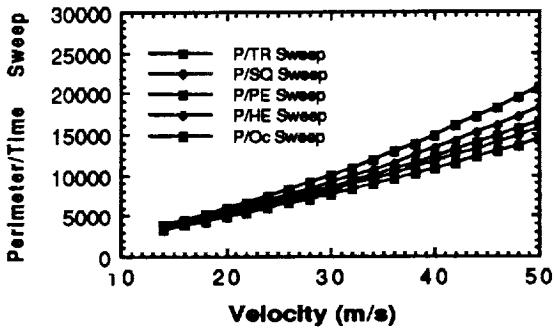

3.4

Fig. 4: Data Aq Time vs Vel (Triangle vs Octagon)

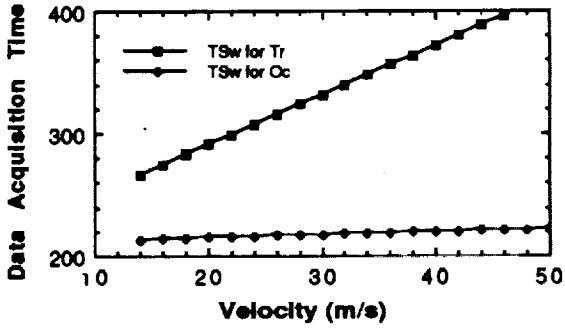

3.5

Fig. 5: Comparison of Data Collection Runs for Triangle and Octagon

Triangle

Data Run	Test Velocities	% Fuel Used
1	46-112 ft/s	65
2	125,138 ft/s	68
3	151 ft/s	55

Octagon

Data Run	Test Velocities	% Fuel Used
1	46-125 ft/s	61
2	138,151 ft/s	53

To explain the data acquisition portion of the mission, one must look at both flight runs. The first flight run will consist of tests at the first 7 test velocities between 46 ft/s and 125 ft/s. This flight will need to consist of 18 3/8 octagonal paths. Each test velocity, which will test 21 different angles of attack on the test section, will take 2 5/8 octagons, with each data leg taking up a side of the octagon. Figure 3.5 shows that the first run will require 61% of the flight vehicle's fuel. The second flight run will test velocities 138 ft/s and 151 ft/s. This run will require 5 1/4 octagonal paths and consume 53% of the alotted fuel. One should note that because of the constraint which states each data acquisition leg will take ten seconds, as the test velocity increases so does the size of the travelled flight path. For example, at the flight velocity of 46 ft/s the perimeter travelled per octagon will be 3,760 feet, while the perimeter travelled for a flight velocity of 151 ft/s will be 16,600 feet.

After completing the data acquisition requirements of the first run, the ground controller will once again assume control of the flight vehicle and guide the MANTA back to the ground.
Once the flight vehicle has returned to the ground, technicians will approach the plane to refuel for the second run, switch battery packs for the onboard data acquisition system, download stored flight data, and begin the pre-flight check for the second run. Once the ground controller clears the MANTA for flight, he will repeat the procedures exactly as with the first flight run.

After the MANTA has finished its second flight run, technicians will approach the plane in order to download onboard data to the computer home station. The MANTA has now finished its mission for a given test section.

3.6 Instrumentation/Data Acquisition System

The MANTA design group set data acquisition as its most important priority. The goals for the data acquisition group were to find the most flexible, lightest, cost efficient system possible. For the mission of the MANTA the data acquisition system (DAS) was required to obtain the lift, drag, and moment of a test specimen located to the front of the plane and then store this data for further use once back on the ground. In conjunction with the previously mentioned tasks, the system would also measure the angle of attack of the plane and the test specimen, measure the static and total pressure of the aircraft's environment, and monitor the output voltage of the battery which would supply the DAS with power.

The actual section properties of the test speciman were obtained from a force sensing system similar to the one shown in Rae and Pope's Low Speed Wind Tunnel Testing. This system uses the output of three strain gauges mounted perpendicularly to one another in order to obtain the lift, drag, and moment of a particular test specimen. This data is measured directly by an internal strain gage force balance system. The force balance is located in the manta's two forward booms. The test specimen will be located between these two forward booms. A single rod running through the middle of the test section will slide into the force balance and be pinned at each end of the rod. This allows for rotation of the rod, and therefore the attached test specimen, through the various angles of attack. A servo is to be calibrated to control the rotation of the test specimen, providing the necessary angle of attack for testing purposes. For the MANTA itself, all of this instrumentation is easily accessible through two hinged doors on the top of both booms. The strain gauges will be configured

just inside of the boom on both sides of the test specimen. A total of six strain gauges will be used.

The force balance is patterned after the NASA force balance design concept. The NASA design is small and provides data collection for three aerodynamic forces, ideal for the manta's mission. This is a simple design and can easily be built by the same manufacturing company of the aircraft.

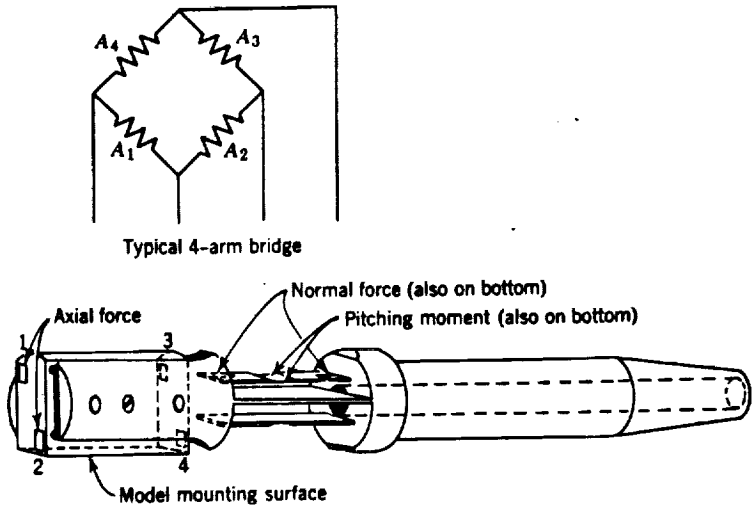

Figure 3.6

The following instrumentation scheme was used to change the raw data gathered by the strain guages into workable material. Each of the strain gauges will be set up in conjuction with transducers which will change the raw data into a given voltage. This voltage will then go through the signal conditioning steps of amplification and filtering in order to remove error from the signal. This signal will then be grouped with the other five signals coming from the strain gauges in a multiplexer. From the multiplexer, the signal will proceed to an analogue - to - digital processor. After the signal has been digitized the signal will be sent to a data storage bank.

Parallel to the system for the input received from the strain guages, there will exist a system for the angle of attack (plane and test specimen), the output voltage of the battery, and the pressure environment of the aircraft. The aircraft will use an inclinometer to measure the angle of attack for both the plane and the test section. Two separate pressure ports will be set up on the forward part of the fuselage. One port will read the static pressure, and the second port will read the total pressure. The battery pack of the system will also have a lead connected to it in order that the controller can have a constant update on the efficiency of the power supply. As with the strain gauge data, each of these subsystems will go through a conditioning process of signal amplification and filtering. These signals will then go through a multiplexer and an analog - to - digital converter. These signals will then branch to two places. As with the section property data, these signals will be stored onboard for later use by the experimenter. However, these signals will also be downlinked to the home base by an FM transmitter in order that the controller can monitor the flight of the MANTA. Figure 3.7 provides a schematic of the entire DAS in order to show the path which the raw data will take in order to become processed and useable by the experimenter.

This DAS system provides a reliable, flexible, and simple way to collect the necessary data for the MANTA research vehicle. Importantly, the system can be built at the reasonable and efficient cost of $4540.00. (See cost breakdown for specifics)

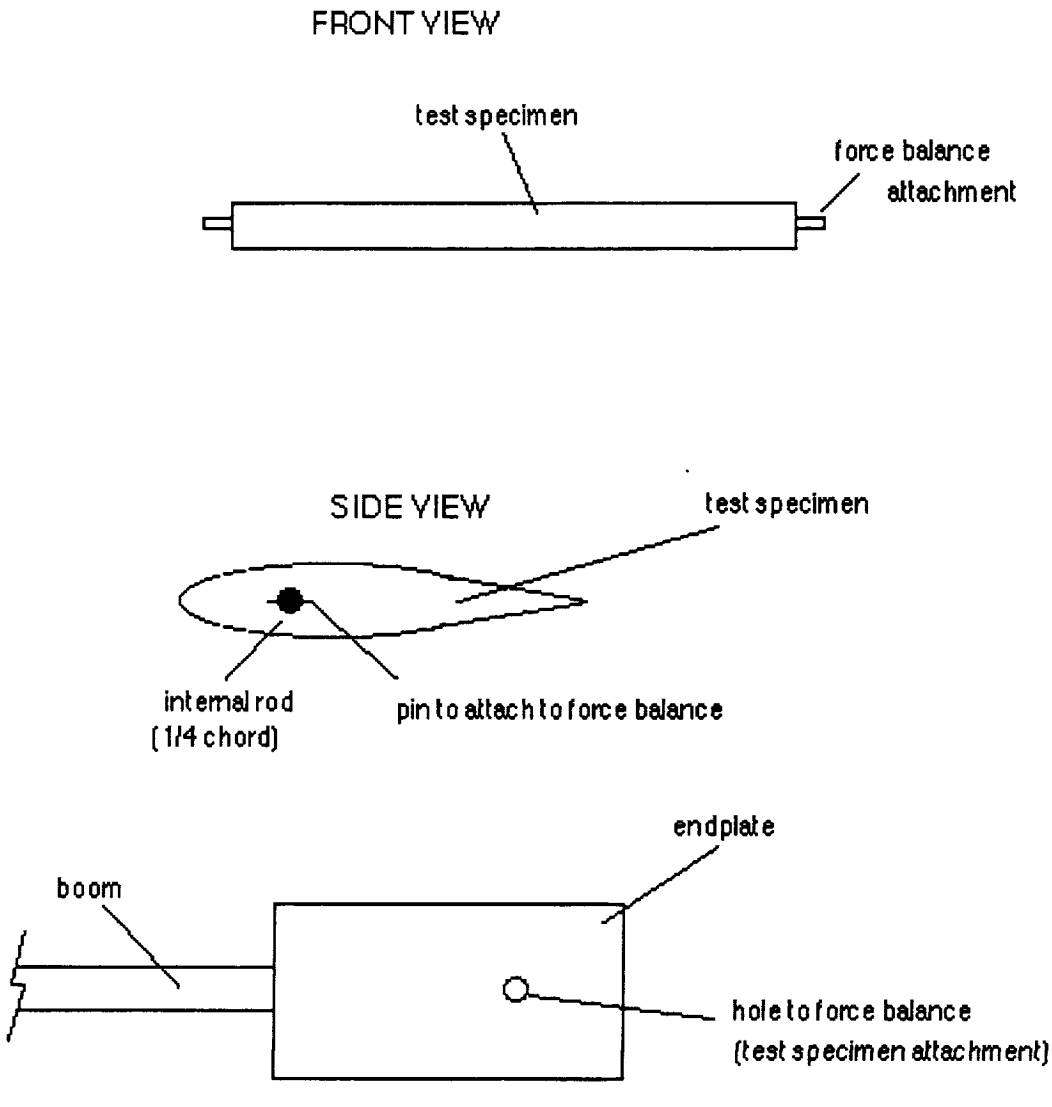
FRONT VIEW
test specimen
force balance
attachment
SIDE VIEW
test specimen
internal rod
(1/4 chord)
pin to attach to force balance
endplate
boom
hole to force balance
(test specimen attachment)

Figure 3.7

Nomenclature

AR	aspect ratio
b	span length
b_{ts}	test section span length
c	chord
Cd	coefficient of drag
Cd_i	induced drag coefficient
Cd_o	zero lift drag coefficient
Cl	coefficient of lift
Cl_{tmax}	tail maximum coefficient of lift
Cl_{wmax}	wing maximum coefficient of lift
Cl_{tsmax}	test section maximum coefficient of lift
C_{mow}	wing zero lift moment coefficient
e	span efficiency factor
l_c	length from center of gravity to test section aerodynamic center
l_t	length from center of gravity to tail aerodynamic center
l_w	length from center of gravity to wing aerodynamic center
S	surface area
S_{ref}	reference area
S_w	wing surface area
S_t	tail surface area

4.1 WING PLANFORM SELECTION

The aircraft's mission profile calls for it to gather data over a wide range of Reynolds numbers, thereby, causing the vehicle to operate at low and high velocities. It is the aerodynamicist's job to design a wing producing high lift and low drag. In the lower velocity range the major contributer to drag is induced drag due to the vortex system created by the wing tips. The wing designed was contrived to limit this significant induced drag in the low velocity sector. The aerodynamic span across a wing is always less than the actual length of the surface because these vortices always leave the wing tips in-board of the wing. An ill-designed wing reduces the effective wing span: the wing will act as if smaller in both area and aspect ratio. Because induced drag is inversely proportional to the aspect ratio, a larger aspect ratio was desired so that the induced drag on the wing would be kept at a low value.

Wing planforms vary from the simple rectangular wing to the strongly tapered wing. Rectangular wings are the easiest to build, yet, are not the best aerodynamically. With a rectangular wing the tip vortex is strong and contributes a large downwash at the outer surface. Sections closest to the tips are influenced the greatest. The section angle of attack is reduced due to the downwash and, consequently, the section c_l is diminished. Thus, the load each portion of the wing carries decreases towards the tips. This gives an unfavorable load distribution.

A strongly tapered wing provides the designer with a wing design at the opposite end of the spectrum in comparison to the rectangular wing. Yet, this type of wing is inefficient and very dangerous. The downwash causes the local angles of attack to increase significantly towards the tips where the area is smaller. The tips are overloaded and stall, giving very undesirable characteristics.

Aerodynamic experiments and calculations show that an elliptical planform area exhibits uniform downwash and presents a perfect load distribution. Yet, tip stall due to laminar separation occurs in the lower end of the Reynolds number range at the outer wing sections. To prevent this a design was chosen closely approximating the ellipse but having greater chord lengths towards the tip. Increasing the chord lengths would increase the Reynolds numbers over the outer wing and reduce the possibility of tip stall.

A trade study looked at wings designed over a wide range of aspect ratios for a given wing loading. A wing loading of 2.58 pounds per square feet combined with the aircraft weight and aspect ratio range from 8 to 15 enabled the span and chord to be determined for each aspect ratio. The taper ratio was then varied for five different values giving the possibility of 40 different wing configurations. After studying the results on wing C_l and Cd_i using the "Lifting Line Program", the optimal design calls for a wing area of 29 square feet with a span of 19.41 feet. The "lifting Line Program" developed by Professor Stephen Batill takes different geometric parameters of the wing and calculates both the coefficient of lift and induced drag coefficient for the various configurations (Figure 4.1).

FIGURE 4.1

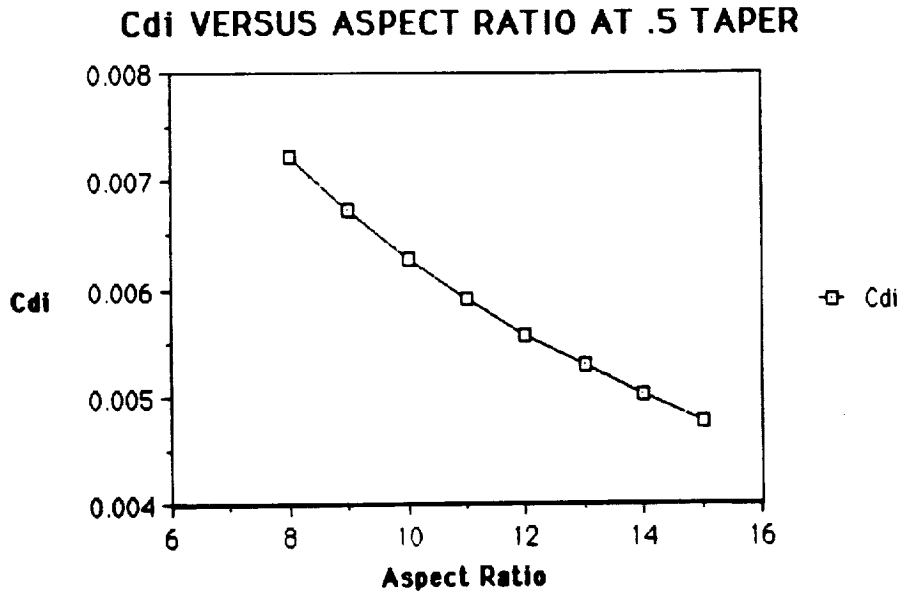

For an aspect ratio of 13, mean chord of 1.49 feet, and taper ratio of .5, the induced drag was significantly lower than at lower aspect ratios (Figure 4.2). At the same time for an aircraft stall speed of 41.18 ft / sec the Reynolds number at the tip is above the corresponding Reynolds number for flow separation. It yields the highest value of the span efficiency factor, e, for a non-elliptical wing planform, approximately equal to 0.95.

ORIGINAL PAGE IS
OF POOR QUALITY

FIGURE 4.2

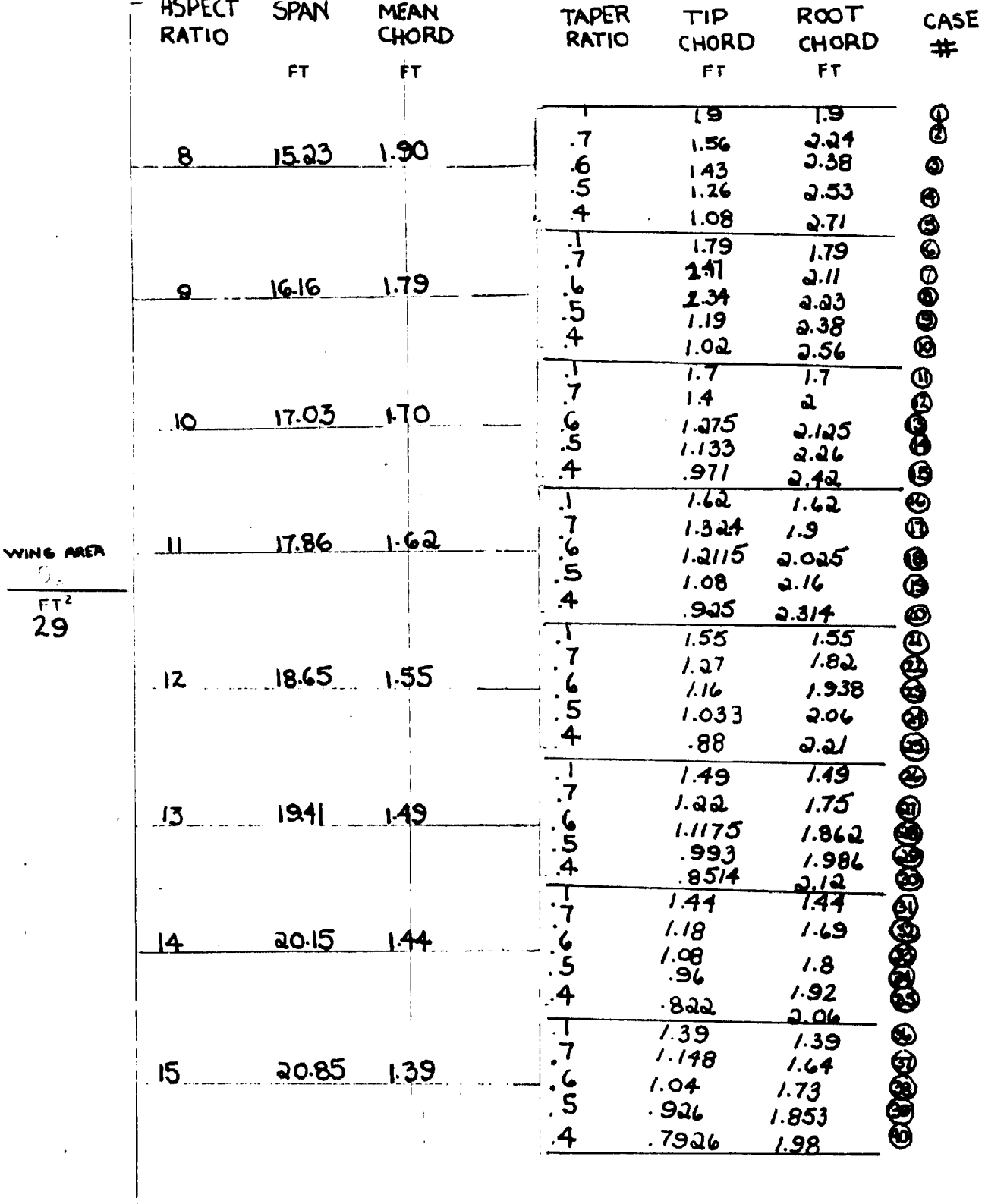

ASPECT RATIO	SPAN FT	MEAN CHORD FT	TAPER RATIO	TIP CHORD FT	ROOT CHORD FT	CASE #
			1	1.9	1.9	①
			.7	1.56	2.24	②
8	15.23	1.90	.6	1.43	2.38	③
			.5	1.26	2.53	④
			.4	1.08	2.71	⑤
			.1	1.79	1.79	⑥
			.7	1.41	2.11	⑦
9	16.16	1.79	.6	1.34	2.23	⑧
			.5	1.19	2.38	⑨
			.4	1.02	2.56	⑩
			.1	1.7	1.7	⑪
			.7	1.4	2	⑫
10	17.03	1.70	.6	1.275	2.125	⑬
			.5	1.133	2.26	⑭
			.4	.971	2.42	⑮
			.1	1.62	1.62	⑯
			.7	1.324	1.9	⑰
11	17.86	1.62	.6	1.2115	2.025	⑱
			.5	1.08	2.16	⑲
			.4	.925	2.314	⑳
			.1	1.55	1.55	㉑
			.7	1.27	1.82	㉒
12	18.65	1.55	.6	1.16	1.938	㉓
			.5	1.033	2.06	㉔
			.4	.88	2.21	㉕
			.1	1.49	1.49	㉖
			.7	1.22	1.75	㉗
13	1941	1.49	.6	1.1175	1.862	㉘
			.5	.993	1.986	㉙
			.4	.8514	2.12	㉚
			.1	1.44	1.44	㉛
			.7	1.18	1.69	㉜
14	20.15	1.44	.6	1.08	1.8	㉝
			.5	.96	1.92	㉞
			.4	.822	2.06	㉟
			.1	1.39	1.39	㊱
			.7	1.148	1.64	㊲
15	20.85	1.39	.6	1.04	1.73	㊳
			.5	.926	1.853	㊴
			.4	.7926	1.98	㊵

WING AREA
S
FT^2
29

4.2 AIRFOIL SELECTION

The airfoil selected was the NACA 23012. This thin airfoil gives higher performance in the lower Reynolds number range in comparison with airfoils having thicker profiles. It also has a high Cl_{max}.

The wing planform characteristics are given in table 4.1

Wing loading = 41.28 oz / ft^2
Wing area = 29.0 ft^2
Aspect Ratio = 13.0
span = 19.41 ft
mean chord = 1.49 ft
taper ratio = .5
Cl = .106 / degree
Cl_{max} = 1.10

TABLE 4.1: Planform Characteristics of Main Wing

4.3 TEST SECTION

The test section of the MANTA was designed to obtain accurate results at the needed Reynolds numbers without producing unwieldy or destabilizing forces and moments.

Both conceptual and analytical methods were used with this purpose in mind. The test specimen was desired to operate over the full Reynolds number range from 40000 to 1 million.

The determination of the minimum chord shall be an empirical process once the MANTA has flown. The primary concern is the error induced in the data by turbulence. Turbulence contains eddies with characteristic lengths varying from a few millimeters to a few kilometers. If eddies are present in the testing environment on the same order of magnitude of the test specimen chord inaccuracy will be present in the data.

This can be reduced by avoiding areas of high turbulence including flying above 300 feet, where there is a calmer freestream. Flights on particularly windy days should be avoided.

There are several relationships to be concerned with in the determination of the maximum test section chord. First, the chord cannot exceed one-half the length of the supporting booms to ensure unconstrained flow over the test section. Also, the lift force generated by the specimen cannot exceed 100 lbs due to instrumentation constraints. Finally, the lift from the test section cannot make the plane unstable. To determine the relationship for max chord, forces and moments on the plane were equated to zero, resulting in:

$$\text{max test section chord} = \frac{C_{mow}S_w + Cl_{tmax}S_t l_t + Cl_{wmax}S_w l_w}{Cl_{tsmax}b_{ts}l_c}$$

From these figures, it is estimated the minimum possilble test section chord would be 3 inches with the maximum test section chord length length at 13 inches.

Another consideration is the placement of the test section. A vortex lattice method

was modified to determine the wing's circulation effects on the test section, varying the wing angle of attack, freestream velocity, and length from the test section aerodynamic center to the wing aerodynamic center. The results are displayed in Figure 4.3. As can be seen, the change in angle of attack on the test section due to circulation is minimal, only approaching .1° near Cl_{max}, low velocities, and with the test section extremely close to the wing. The change in angle of attack on the test section will never exceed .05° as long as the distance from the wing aerodynamic center to the test section aerodynamic center is three chord lengths or greater.

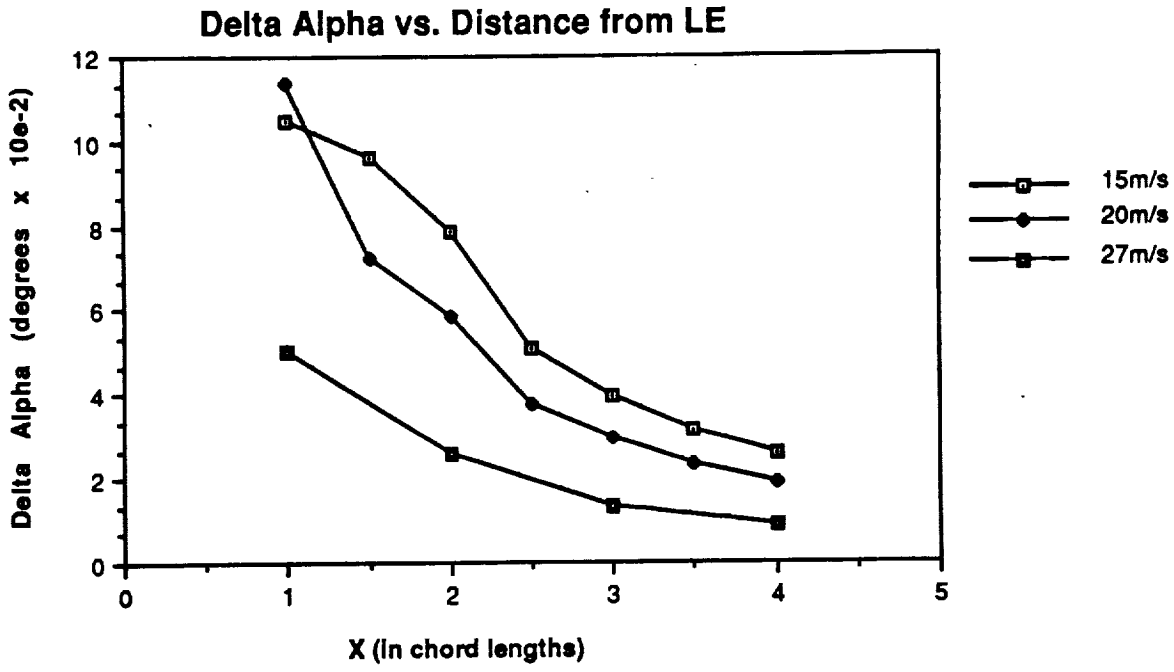

Figure 4.3

4.4 DRAG PREDICTION

The aerodynamic drag experienced by the MANTA was estimated using classical techniques. It involves summing both the drag coefficient at zero lift and the induced drag coefficient due to lift.

The zero lift drag can be estimated by dividing the aircraft into its basic components and finding their zero lift drag coefficients. The zero lift drag can then be estimated using the formula:

$$Cd_0 = E(Cd_0 S_{ref}) / S_{ref}$$

Component	Cdo	$S_{ref}(ft^2)$
wing	.007	29
fuselage	.080	.3937
vertical stabilizer	.008	.9022
horizontal stabilizer	.008	2.72
test section	.0066	6.56
endplates	.008	1.44
nacelle	.12	.131
landing gear	.003	.03

TABLE 4.2: Cd_0 and S_{ref} for aircraft components

Expanding the equation for zero lift calculation using the values listed in Table 4.2 gives

$$Cd_o = .0115$$

In order to estimate the induced drag coefficient due to lift, it was assumed that the induced drag was primarily influenced by the wing. This is a reasonable approximation as the other components of the aircraft contribute only a small portion to the lift and are normally neglected.

The general expression for the induced drag coefficient is as follows:

$$Cd_i = Cl^2 / (3.1415ARe) = CL^2 / ((3.1415)(13)(.95))$$
$$= .0257$$

Combining both the induced drag coefficient and the zero lift drag coefficient gives the following expression for the coefficient of drag for the aircraft:

$$C_d = .0115 + .0257C_l^2$$

5.0 STRUCTURES

5.1 INTRODUCTION

The structures analysis of the MANTA is broken down into several different sections. The three main sections are 1) the wing structure,
2) the fuselage structure, and 3) the data acquisition boom structure. Along with these areas, two other sections were investigated; 4) the weight and balance (center of gravity) and 5) materials selection. The following discussion will present these areas individually and will relate them to the aircraft design itself.

5.2 STRUCTURAL GEOMETRIES

As a prelude to the discussion on the wing structure, it is important to look at structural geometries in general. The design of the aircraft structure is extremely complicated and can become extremely involved. There are many conditions that must be investigated in designing a structure; normal stresses, shearing stresses, and torsional effects. (Figure 5.1) All of these conditions could present serious structural problems if they exceed the allowable levels. This includes the possibility of structural failure.

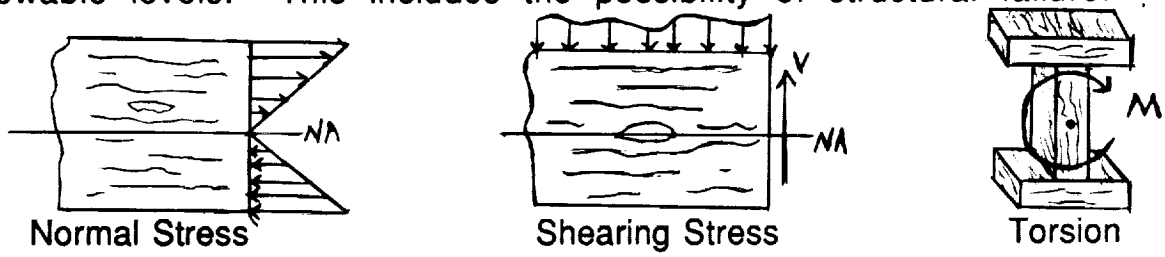

Figure 5.1

The goal in designing an aerodynamic structure is to obtain the maximum strength requirements while reducing the weight as much as possible. This involves the analysis, comparison, and selection of structural geometries. Several such geometries are depicted in Figure 5.2.

Rectangular

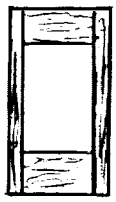

"Box"

I-Beam

Figure 5.2

The rectangular geometry is a basic and commonly used geometry for structural members such as wing and fuselage spars. The "box" geometry involves two rectangular sections that are "sandwiched" by side plates. The I-Beam geometry is also common and is comprised of a central rectangular section. These sections are capped on the top and bottom by additional rectangular sections.

The analysis of structural sections and structural geometries such as these is greatly simplified through the use of models. The analysis of entire structural elements could become extremely involved and would require advanced technical tools such as computer aided finite-element analysis. In light of this, simple elementary models can be studied in order to yield insight into the behavior of actual, more complex structures.

For the design of the MANTA, a parametric trade study was conducted that cross-compared these simple geometries. This involved comparing the strength and weight of the different geometries and the feasibility of using them in specific parts of the aircraft. This was done in order to find which geometry would provide the proper strength, would weigh the least, and would fit and function well in the sections of the aircraft structure. In the following discussion, the most effective structural geometries will be presented along with the role it will serve.

5.3 THE WING STRUCTURE

The main concern in the design of the wing is the shearing forces and bending moments that will result from the wing loading.

These quantities are induced by the lift, drag, and wing weight distributions, as well as other loads such as the engine weight. This scenario is depicted in Figure 5.3a.

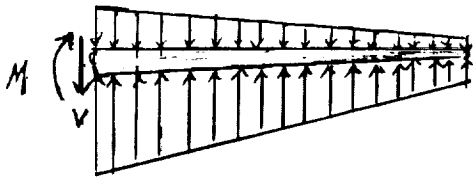

Figure 5.3a

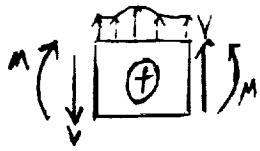

Figure 5.3b

The shear and bending moment on the wing was calculated from a simple force and moment balance. Figure 5.3b defines the convention that was used in formulating the following equations:

$$V(x) = -\frac{1}{2}(w_0 + w)x + \frac{1}{2}(L_0 + L)x \qquad \text{Equation 5.1}$$

$$M(x) = -(2w_0 + w)\frac{x^2}{6} + (2L_0 + L)\frac{x^2}{6} \qquad \text{Equation 5.2}$$

Both of these equations treat the wing tip as the origin (X=0) and move in toward the root where X=L.

The data for the wing loading and the resulting stress and bending moments were obtained through simple calculations and engineering estimations. The total lift on the wing semi-span was based on an airfoil section lift coefficient of .015 and an angle of attack of 5 degrees. This yielded a value of approximately 8 lbs. The weight of the wing semi-span was estimated to be 4 lbs. Since the wing airoil section is constant along the span and the wing tapers linearly from root to tip, a linear distribution was assumed. This data is given in Figure 5.4.

The wing loading distribution, the shear distribution, and the bending moment distribution (as functions of position along the wing) are depicted in Figures 5.5, 5.6, and 5.7. As can be seen from the diagrams, all of the quantities are maximum at the root and decrease along the semi-span. From this analysis, the maximum shear force was determined to be 10 lbs and the maximum bending moment to be

80 ft-lbs. It is this location (wing root) of maximum stress and bending moment that is of primary concern in the design process and is the point that will dictate the design.

The actual structural configuration of the wing is depicted in Figure 5.8. The loading on the wing is carried by the spars that run spanwise along the wing. There is a leading edge spar, a trailing edge spar, and a main load- carrying spar at about the c/4 position. This is the point of maximum wing

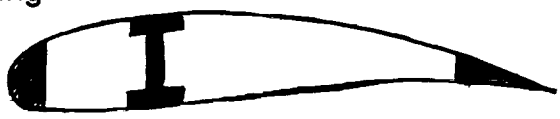

Figure 5.8

thickness. The leading and trailing edge spars are solid rectangular-type geometries. The main spar was chosen to have an I-Beam geometry.

The leading and trailing edge geometries were selected because the solid geometry lends to shaping and fitting into curved and odd shaped areas that are dictated by the airfoil shape. The I-Beam geometry gives a high strength beam that is also light weight.

5.4 THE FUSELAGE STRUCTURE

The fuselage structure for the MANTA is unique in its shape and composition. As can be seen from the sketches of the aircraft, the fuselage is flat so as to accomodate the data acquisition booms. Along with this, the booms on the front of the MANTA support heavy equipment. It is extremely important that the fuselage structure be strong enough such that it can support the payload.

The main fuselage is comprised of long runners that travel from the front of the fuselage to the tail. The shape and torsional rigidity of the rectangular fuselage is maintained by rectangular bulkheads that are positioned along the length of the fuselage. As shown in Figure 5.9, the runners lie along the corners of the fuselage, held in place by the bulkheads.

The outside of the fuselage is covered by thin wood plates and

monocoating. Additional composite pieces are added to give strength and toughness.

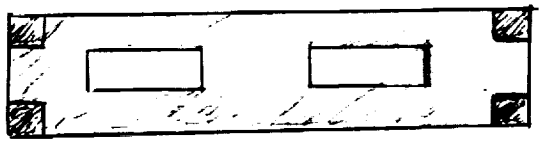

Figure 5.9

The data acquisition booms are configured much the same as is the fuselage. (Figure 5.9) The corners of the booms are composed of wood runners that are held together by bulkheads. The main structural concern in regard to this section is the way in which it is secured to the main fuselage. This is done by passing excess runner through both sections. This in turn allows them to be bolted to a common bulkhead; the same bulkhead that is used as the reference for center of gravity calculations. This configuration is depicted in Figure 5.10.

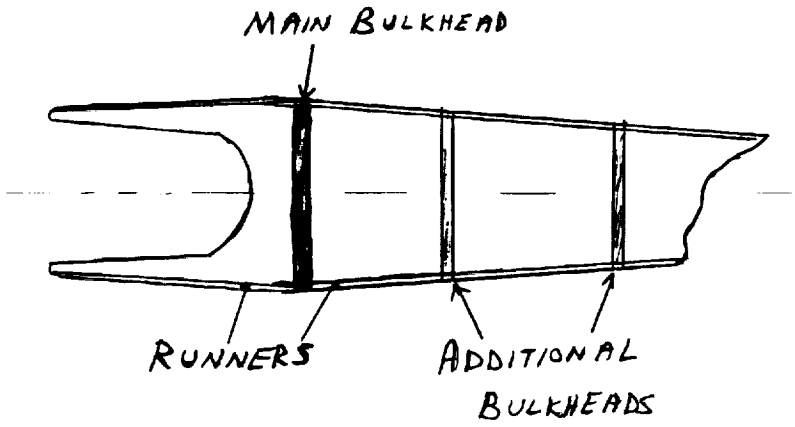

Figure 5.10

Trade Data

Calculation of Shear and Bending Moment along semi-span of a wing

Semi-Span= 9 ft. Root... W= .1 lb/ft L= 5 lb/ft
Planform is linearly tappered Tip... Wo= 1 lb/ft Lo= .55 lb/ft

	X	Shear (lb)	Moment (ft-lb)
Wing Tip >>>	0	0	0
	0.25	0.05625	-0.00625
	0.5	0.1125	-0.025
	0.75	0.16875	-0.05625
	1	0.225	-0.1
	1.25	0.28125	-0.15625
	1.5	0.3375	-0.225
	1.75	0.39375	-0.30625
	2	0.45	-0.4
	2.25	0.50625	-0.50625
	2.5	0.5625	-0.625
	2.75	0.61875	-0.75625
	3	0.675	-0.9
	3.25	0.73125	-1.05625
	3.5	0.7875	-1.225
	3.75	0.84375	-1.40625
	4	0.9	-1.6
	4.25	0.95625	-1.80625
	4.5	1.0125	-2.025
	4.75	1.06875	-2.25625
	5	1.125	-2.5
	5.25	1.18125	-2.75625
	5.5	1.2375	-3.025
	5.75	1.29375	-3.30625
	6	1.85	-2.1
	6.25	1.90625	-2.53125
	6.5	1.9625	-2.975
	6.75	2.01875	-3.43125
	7	2.075	-3.9
	7.25	2.13125	-4.38125
	7.5	2.1875	-4.875
	7.75	2.24375	-5.38125
	8	2.3	-5.9
	8.25	2.35625	-6.43125
	8.5	2.4125	-6.975
	8.75	2.46875	-7.53125
Wing Root >>>	9	2.525	-8.1

Figure 5.4

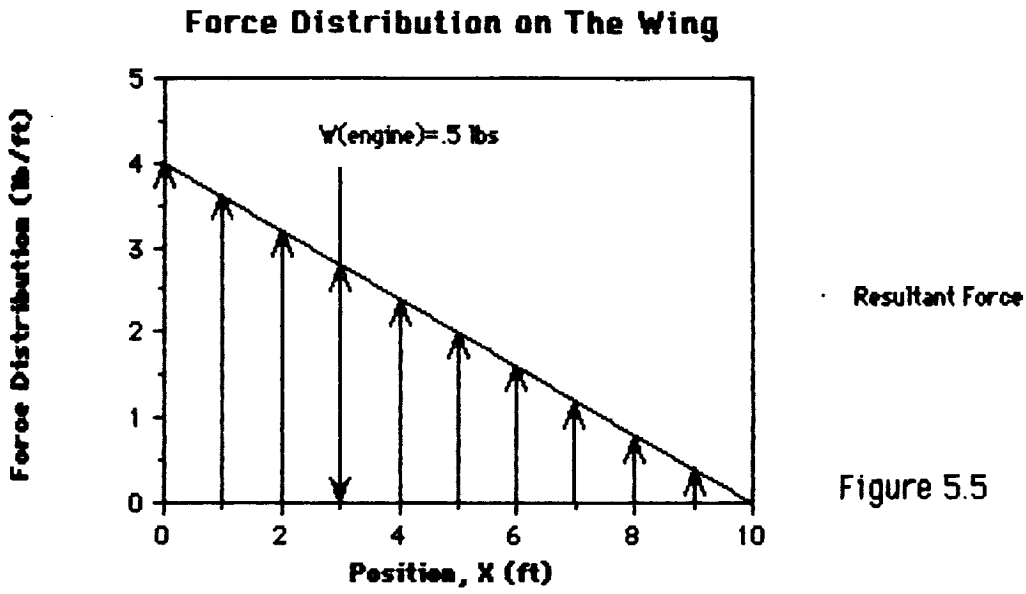

Figure 5.5

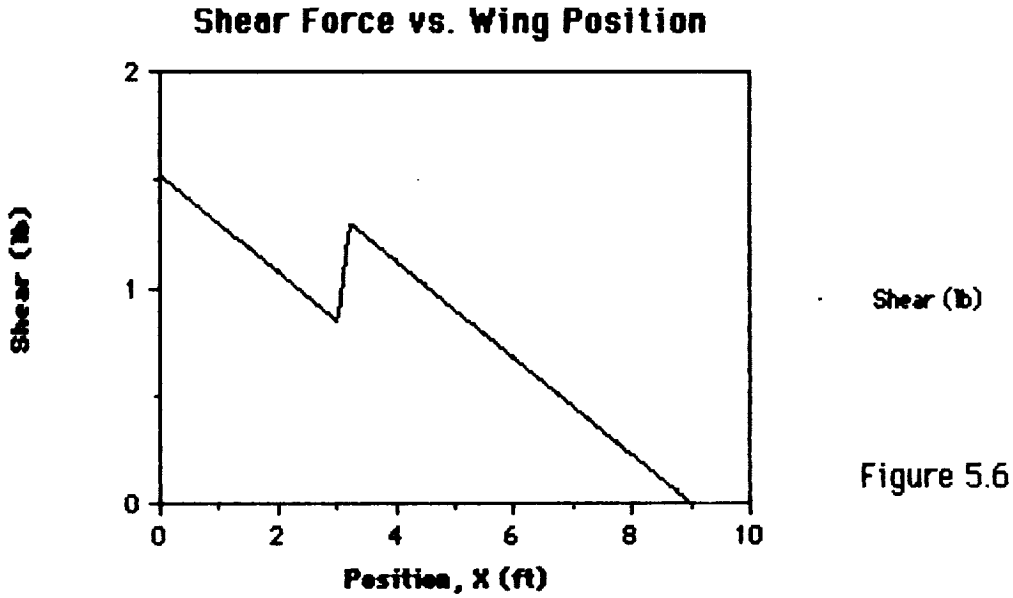

Figure 5.6

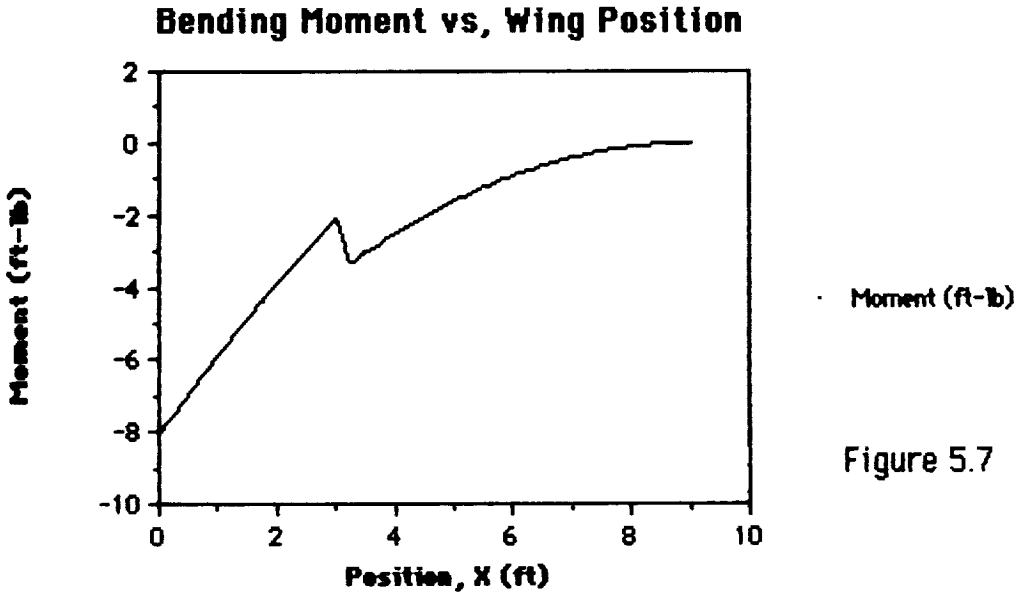

Figure 5.7

5.5 CENTER OF GRAVITY

The location of the center of gravity is a pivotal element in the design of an aircraft. Poor weight balance in relation to the aircraft's aerodynamic center will cause the aircraft to be unstable and basically incapable of maintaining stable flight. It is extremely difficult, with any degree of accuracy, to locate the center of gravity in the theoretical stage of design. The goal, though, was to make a sound engineering estimation of its approximate location.

This goal was achieved through a piece-by-piece analysis, weight and balance approach. The MANTA was subdivided into ten separate elements:
the wing, the forward fuselage section, the rear fuselage section, the engines, the horizontal stabilizer, the vertical stabilizer, the data acquisition equipment, the fuel, and the control system. Each of these elements were given prospective weights and locations in reference to a bulk head in the front of the aircraft, as shown in Figure 5.11. Also shown are the ten separate elements of the MANTA. From the relationship

$$Xcg = \Sigma (Xi * Wi) / \Sigma (wi) \qquad \text{Equation 5.3}$$

where i varries from one to ten. The weight/location data and results of this analysis are presented in Figure 5.12.

As the results indicate, the center of gravity is located directly behind the C/4 position of the wing; 1.2 feet behind the bulkhead. For a stable aircraft, the center of gravity needs to be as far forward of the aircraft's aerodynamic center as possible. The theoretical projection for the MANTA is that the center of gravity location is not a problem. If some adjustments are needed, the location of the payload can be adjusted or ballast can be added.

Center of Gravity Calculations for the MANTA

Aircraft Component	Weight (lbs)	Position	Wt * X
Wing	10	0.5	5
Engines (2)	1	0.2	0.2
Fuselage (forward)	6	1	6
Fuselage (aft)	4	4.33	17.32
Booms	1	-1	-1
Horizontal Stabilizer	1	9	9
Vertical Stabilizer	1	9	9
Data Acquisition Equipment	5	-1	-5
Fuel	1	1	1
Control System (servos, etc)	2	1	2
	Total Weight =	32	
	Total W*X=	43.52	

Therefore, Xcg 1.36 ft

Figure 5.10

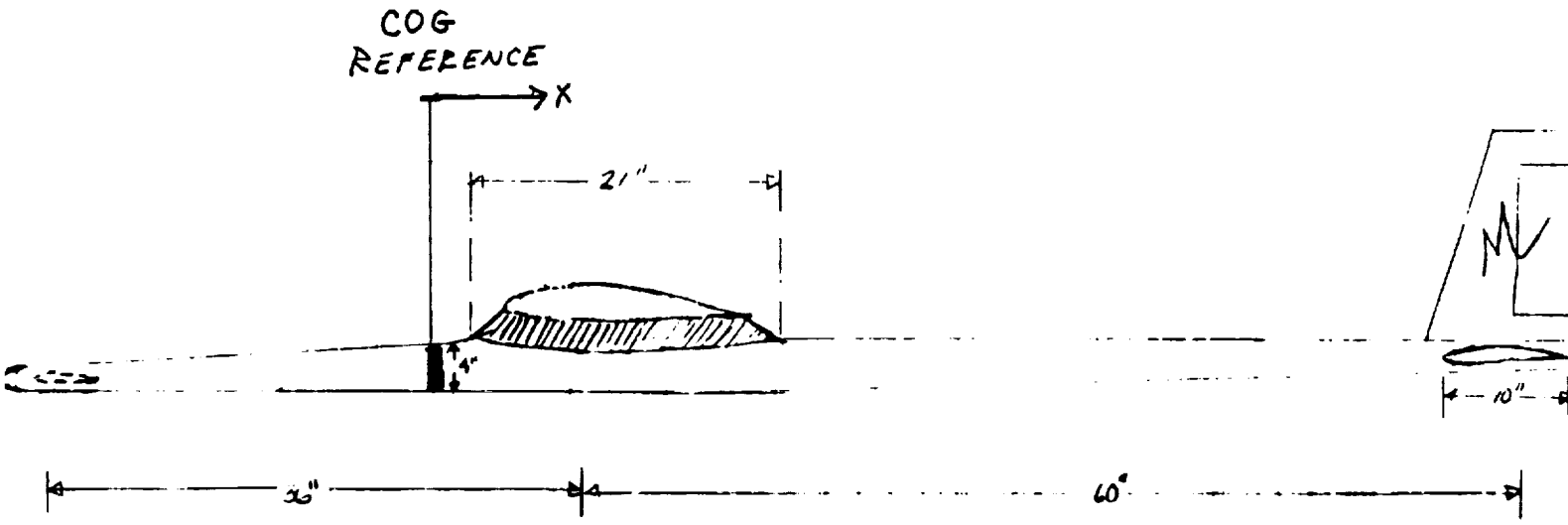

Figure 5.11

X	W	Wo	L	Lo
9	0.5	0.05	0.8	0.2
8.75	0.5	0.05	0.8	0.2
8.5	0.5	0.05	0.8	0.2
8.25	0.5	0.05	0.8	0.2
8	0.5	0.05	0.8	0.2
7.75	0.5	0.05	0.8	0.2
7.5	0.5	0.05	0.8	0.2
7.25	0.5	0.05	0.8	0.2
7	0.5	0.05	0.8	0.2
6.75	0.5	0.05	0.8	0.2
6.5	0.5	0.05	0.8	0.2
6.25	0.5	0.05	0.8	0.2
6	0.5	0.05	0.8	0.2
5.75	0.5	0.05	0.8	0.2
5.5	0.5	0.05	0.8	0.2
5.25	0.5	0.05	0.8	0.2
5	0.5	0.05	0.8	0.2
4.75	0.5	0.05	0.8	0.2
4.5	0.5	0.05	0.8	0.2
4.25	0.5	0.05	0.8	0.2
4	0.5	0.05	0.8	0.2
3.75	0.5	0.05	0.8	0.2
3.5	0.5	0.05	0.8	0.2
3.25	0.5	0.05	0.8	0.2
3	0.5	0.05	0.8	0.2
2.75	0.5	0.05	0.8	0.2
2.5	0.5	0.05	0.8	0.2
2.25	0.5	0.05	0.8	0.2
2	0.5	0.05	0.8	0.2
1.75	0.5	0.05	0.8	0.2
1.5	0.5	0.05	0.8	0.2
1.25	0.5	0.05	0.8	0.2
1	0.5	0.05	0.8	0.2
0.75	0.5	0.05	0.8	0.2
0.5	0.5	0.05	0.8	0.2
0.25	0.5	0.05	0.8	0.2
0	0.5	0.05	0.8	0.2

Figure 5.12

5.6 MATERIALS SELECTION

The material used for the MANTA's structure is comprised mainly of wood. The utility of wood comes in its light weight, its strength, and its ease of fabrication. Wood works well as a load carrying material that will also flex in the event of extreme stress. Other materials were also looked at. Some of the candidate materials included aluminum, fiberglass, and composites. It was decided that some fiberglass and composites would be used to provide impact strength on certain parts.

The major load-carrying members are made from a hard wood such as spruce and plywood. The remaining structural elements are constructed from balsa. The entire structure is coated with a plastic monocoat that gives it a rigidity for torsional effects. Fiberglass wrapping is used at major structural joints in order to provide strength and continuity in the structure. This is the case for the wing joints and areas around the boom arrangement.

In the interest of survivability and toughness, wing tips, leading edges, and potential impact points are sheeted with a tough material. This material might be plastic or a composite of sorts. Not enough is known about material properties and behavior in order to provide definite design plans. This is an area that needs to be investigated in depth; to an extent that is beyond the scope of this analysis.

6.0 Longitudinal Stability System Design

When the MANTA was first conceived one of the major areas of concern was the effect of the test section on the aircraft's longitudinal stability. During the tests, this section could produce significant lift and highly destabilizing moments. It was therefore necessary to design a longitudinal control system that could trim the aircraft in steady level flight throughout the entire test regime. The tests are to be performed at various Reynolds numbers and angles of attack. Thus, the test specimen will vary in size and angle of attack in order for the testing range to be satisfied. This will lead to a variation in the destabilizing moments. However, the problem is simplified if the longitudinal control system is designed about the most destabilizing conditions.

In modeling the test section several assumptions were made. First, the test section moment arm from the center of gravity was set at 3 feet. This was based on the desire to minimize the circulation effects from the wing on the tests. A distance of 3 feet produced insignificant circulation effects. Since the wing is typically close to the center of gravity, the arm length was set at three feet. The maximum chord needed to reach the upper portion of the Reynolds number range was 1.0833 feet. Since the maximum test span is 1 foot the maximum volume ratio of the test section was set.

A second area of assumption was the aerodynamic characteristics of the test section. Since two dimensional data is to be modeled during the tests, it is reasonable to expect a two dimensional lift slope. The theoretical maximum lift slope is .1097 per degree. This lift slope was assumed for the test section. In addition the test specimen was modeled to have zero lift at zero angle of attack, to separate at positive and negative 20 degrees and to have a moment coefficient of -.05. These assumptions will set the most destabilizing case of the test regime to be -20 degrees. It is this point about which the MANTA's longitudinal stability system was designed.

The design of the horizontal stability system involves the selection of certain

parameters:

1. Selection of stabilizer airfoil section
2. Selection of tail moment arm
3. Selection of horizontal tail area
4. Selection of horizontal tail aspect ratio

The factors that will constrain the selection of these parameters are:

1. Acceptable static margin
2. Drag minimization
3. Weight minimization

The capabilities that the system must satisfy are:

1. Ability to trim aircraft in steady level flight throughout test regime.
2. Have enough control power to trim aircraft through acceptable angle of attack range.

6.1 Selection of Tail Airfoil Section

The selection of the airfoil section for the horizontal stabilizer was constrained primarily by the static margin and preliminary estimates of the center of gravity location. Typical desired static margins range from .05 to .10. The MANTA's static margin will vary depending on the test specimen size and aerodynamic lift slope. The static margin decreases with the increase of either of these parameters. In the design of the stabilization system, both of these were set at their maximum allowable

extremes. Thus, the static margin of the aircraft during the test will be at least the design value. Based on this, a static margin of .05 was chosen as the design point since it is the minimum value of the desirable range.

The airfoil section for the stabilizer affects the center of gravity location. The higher the stall angle of the stabilizer, the closer to the aerodynamic center of the wing the center of gravity needs to be to achieve the .05 static margin. Preliminary estimates indicate the center of gravity of the MANTA to be approximately 2 inches behind the aerodynamic center of the wing (equivalent to 36% chord from the leading edge of the wing). A stall angle of -8 degrees yields the center of gravity to be at this point (see Figures 6.1 and 6.2). Thus, the center of gravity does not need to be adjusted with weight by adding ballast if a stall angle of -8 degrees is used. In addition, the higher the stall angle, the smaller the tail volume ratio needs to be, which also reduces weight and drag. Thus, the airfoil section suggested is the NACA 0009 because it exhibits such a stall angle.

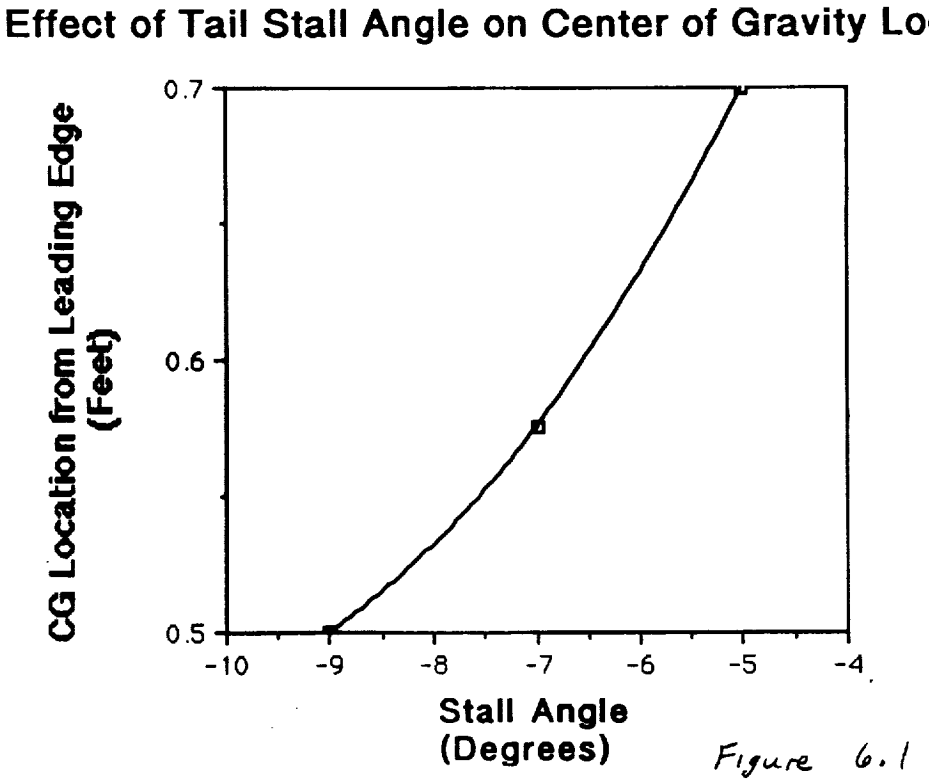

Figure 6.1

6.2 Tail Surface Size, Moment Arm Length and Aspect Ratio Selection

With the selection of the NACA 0009 airfoil section, the effect of the tail moment length and and aspect ratio on tail surface size were investigated. Aspect ratio was varied throughout a typical range from data base of 3 to 4.5. The tail moment arm was varied from 5 feet to the preliminary design estimate of 7.833 feet. Results indicate that low aspect ratio and low moment arm increase surface area (see Figure 6.3). Thus, a large moment arm and high aspect ratio tail would seem to be desired. However, although investigation into the effects of these two parameters on drag indicate this is true for aspect ratio, it is not the case as far as moment arm is concerned (see Figure 6.4). Increase of moment arm increases drag. This is obviously undesirable. Thus a small moment arm and high aspect ratio are desirable.

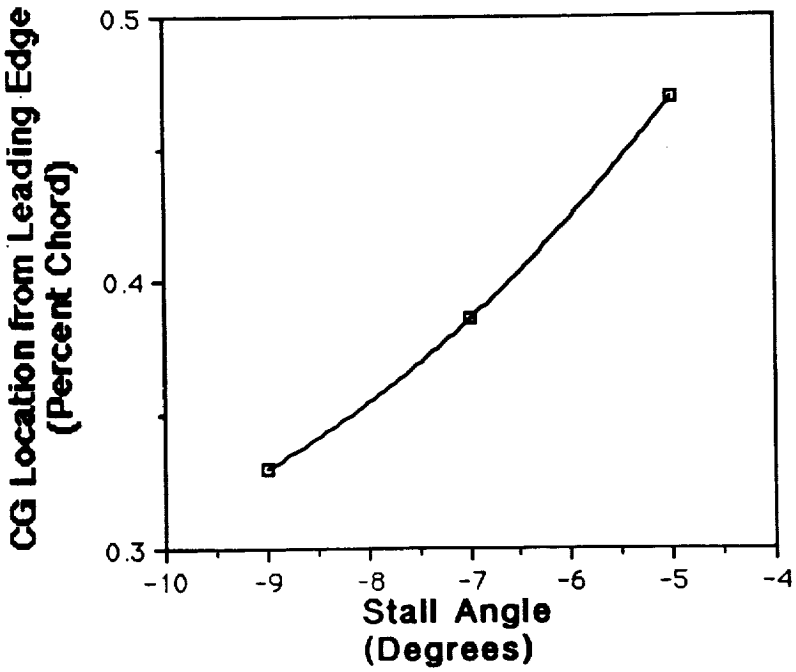

Note that CG positions based on average values for these angles of attack. However, other parameter variation does not significantly vary the location.

Figure 6.2

Effect of Tail Moment Arm and Aspect Ratio on Surface Area

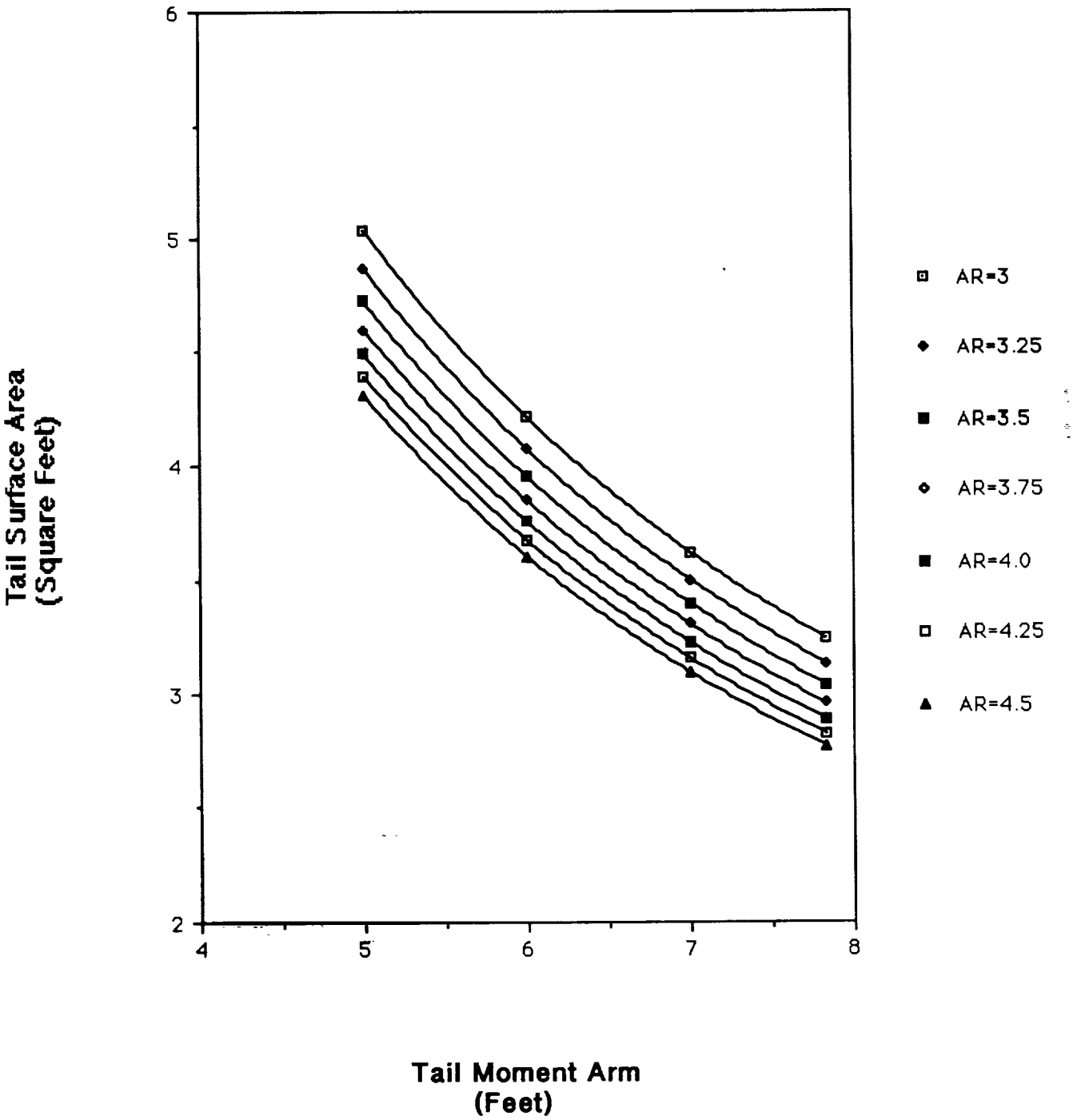

Figure 6.3

Effect of Aspect Ratio and Tail Length on Drag

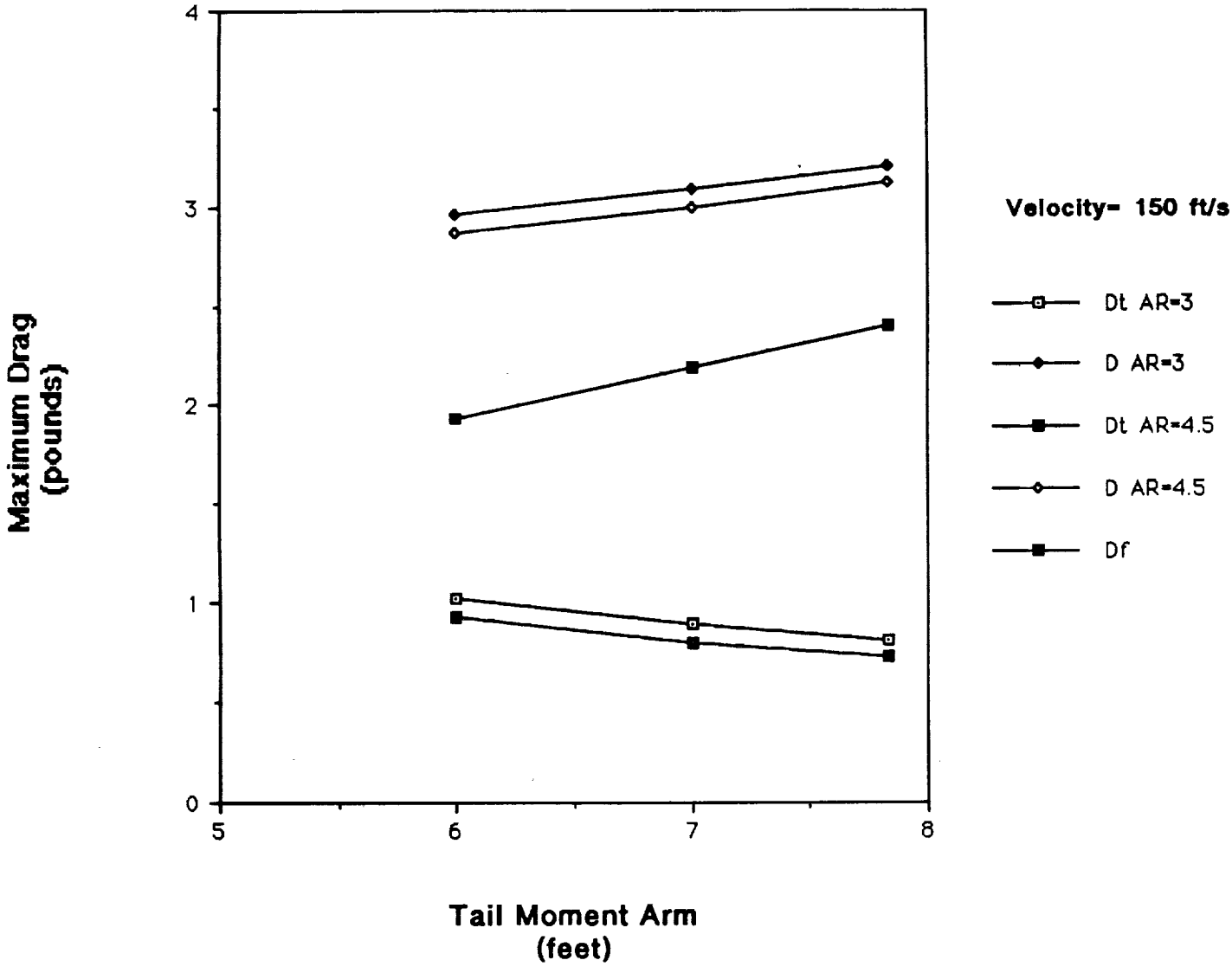

Figure 6.4

6.3 Performance of the Horizontal Stability System

Aside from being able to trim the aircraft in steady level flight, the system must also be able to trim the aircraft throughout an acceptable wing angle of attack range. A major concern is trimming the aircraft during takeoff when the aircraft is flying at low speeds and high angle of attack. However, investigation shows that if the test section is set at zero incidence, there is plenty of control power to stabilize the aircraft. The required stall angle of the tail to trim the aircraft at takeoff (maximum Cl) was calculated for various tail moment lengths. Results show the tail to have sufficient control power throughout the moment arm range (see Figure 6.5). In addition the minimum allowable angle of attack of the wing that can be trimmed was calculated as a function of tail moment arm (see Figure 6.6). Overall results indicate that the MANTA can be trimmed at wing angles of attack of approximately -11 to +18 degrees if the test section is at zero angle of incidence.

Figure 6.5

Effect of Tail Moment Arm on Stall Angle Required for Takeoff

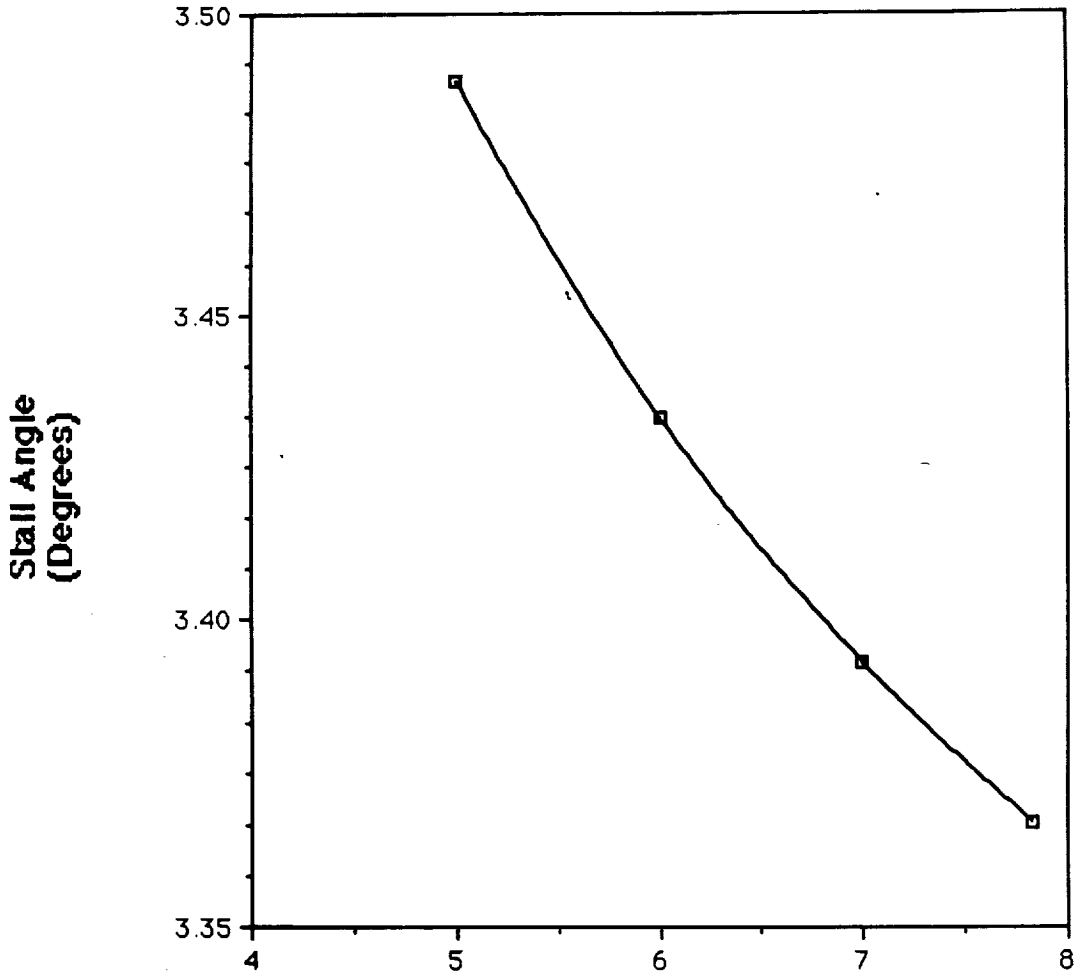

Figure 6.6

Effect of Tail Moment Arm on Minimum Angle of Attack

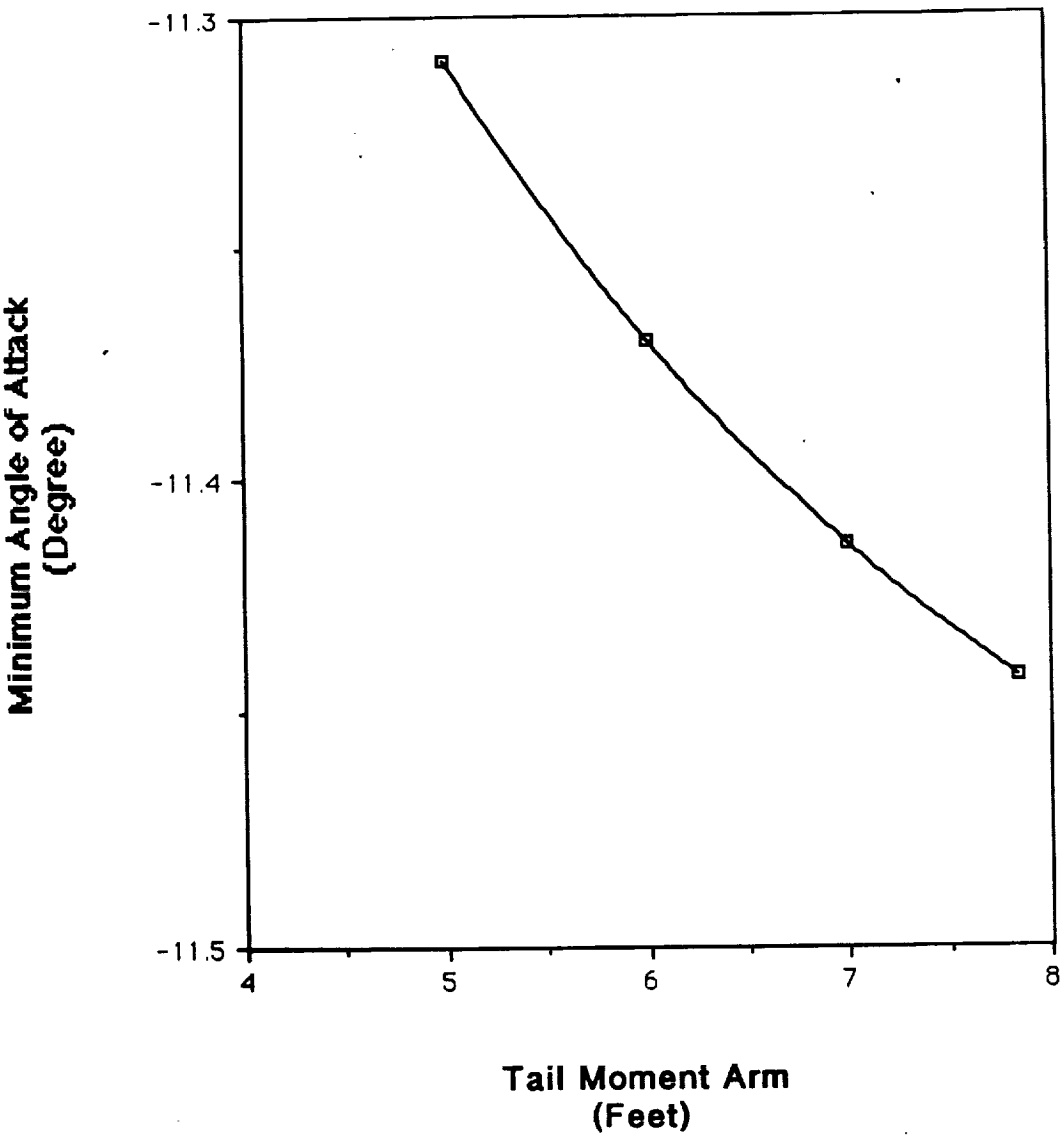

6.4 Assumptions and Considerations

During the investigation of the parameters, several assumptions were made:

1. Any contribution to longitudinal moment from components off line in the vertical direction were ignored. Thus, all components were assumed in the same horizontal plane. This assumption neglects such factors as longitudinal moments from the engines and the wing which result from these components being above or below the center of gravity.

2. A tail to free stream dynamic pressure ratio of .8 was assumed. Originally this seemed reasonable as typical values range from .8 to .9 and there was concern about loss due to wake from the test section. However, with the engines mounted close to the fuselage, slip stream effects will probably increase the ratio to above one.

3. Variation in center of gravity location during flight due to fuel loss was neglected. Fuel makes up a small component of the aircraft's weight and thus the center of gravity is not expected to vary considerably. In addition, the design static margin of .05 should allow for such variation and still keep the aircraft stable.

4. Since the drag was not neglected, the change in moment with angle of attack is not linear. The static margin is based directly on this slope. The static margin was therefore based on the slope of the curve at trim conditions.

5. Note that the drag variation with tail moment arm does not include the drag from horizontal stabilizer. However, the trend of increase in drag with moment arm is expected to continue due to the large surface area of the rear fuselage.

6. An additional consideration with regard to the tail moment arm is that the weight of the aircraft will increase with the length. In addition, a long moment arm may present structural problems.

6.5 Basic Results

Based on the analysis, the following characteristics will allow a satisfactory horizontal stability control system and allow the following performance:

Specifications

Tail Aspect Ratio=4.5

Airfoil Section: NACA 0009

Moment Arm: 5-7.833 feet

Horizontal Planform Area: 4.3 to 2.77 square feet (respective to moment arm)

Performance

Trim wing angles of attack between -11 and +18 degrees with test section at zero incidence.

Maintain steady level flight throughout test regime for airfoil sections of types within model constraints.

7.0 PROPULSION SYSTEM

The selection of the propulsion system for the MANTA flight vehicle was limited to a propeller system at the very beginning. A propeller has better efficiency and endurance than both gas turbine and rocket propulsion for the low flight speeds at which MANTA will operate. The engines had to be light but provide adequate power to meet very stringent flight velocity requirements. Two engines were necessary because of the conceptual design selected; they had to be mounted on the wings simply to minimize their disturbance of the air over the test specimen. The approach to propeller design involved maximizing the efficiency of the airscrews over a large flight velocity range. MANTA's propulsion system basically has two goals: to provide adequate power to fly the aircraft and to enable the aircraft to fly at the high velocities needed to attain the highest test specimen Reynolds number required in steady, level flight.

7.1 Propeller

In designing the propeller, three basic objectives were kept in mind. First, the propeller needed to have a good efficiency over the flight velocity range

$$65 < V < 155 \text{ ft/s.}$$

Second, adequate power was needed to clear a 50 ft high obstacle on takeoff in less than 300 ft. Most importantly, the propellers had to be able to maintain steady, level flight at 140 ft/s, the velocity needed for the test specimen to reach a Reynolds number of 1 million.

There were several constraints on the propellers which were considered throughout the design. Neither propeller could be above a reasonable size for this type of aircraft. After searching a database of similar aircraft, this upper limit was judged to be a 3 ft diameter. Also, rotational speed had to be kept below 3000 rpm to avoid tip stall and loss of thrust. The final constraint was that the propellers must be of fixed pitch. While a variable pitch system is possible, it also adds more weight to the aircraft. In a flight vehicle of MANTA's class, minimum weight is one of the most important priorities.

Analysis of the effect of propeller pitch on efficiency was conducted over a range of flight speeds from 65 to 165 ft/s. Figure 7.1 gives the efficiency as a function of advance ratio. This was used to select the 75% radius pitch angle of 40 degrees, which

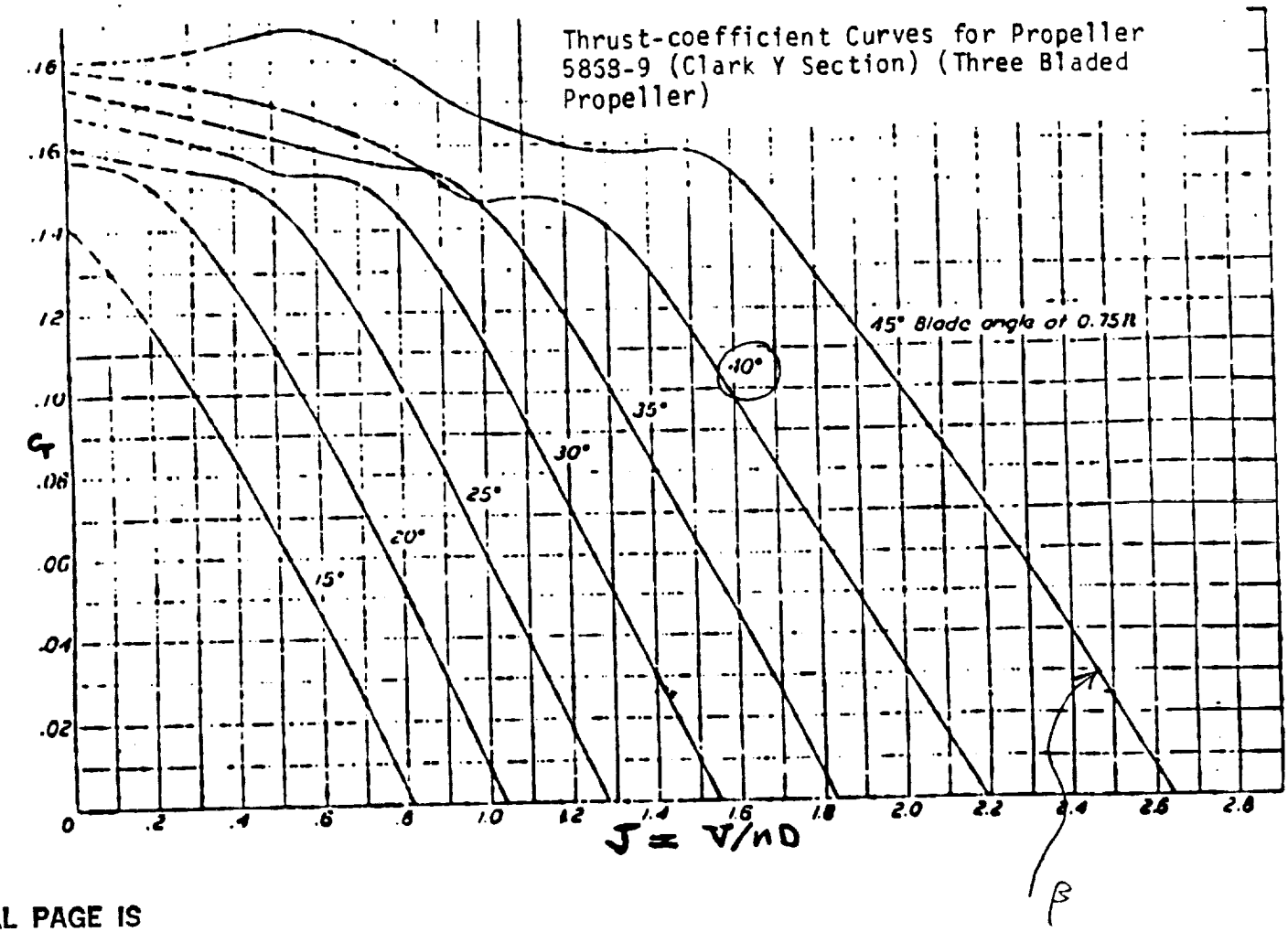

ORIGINAL PAGE IS
OF POOR QUALITY

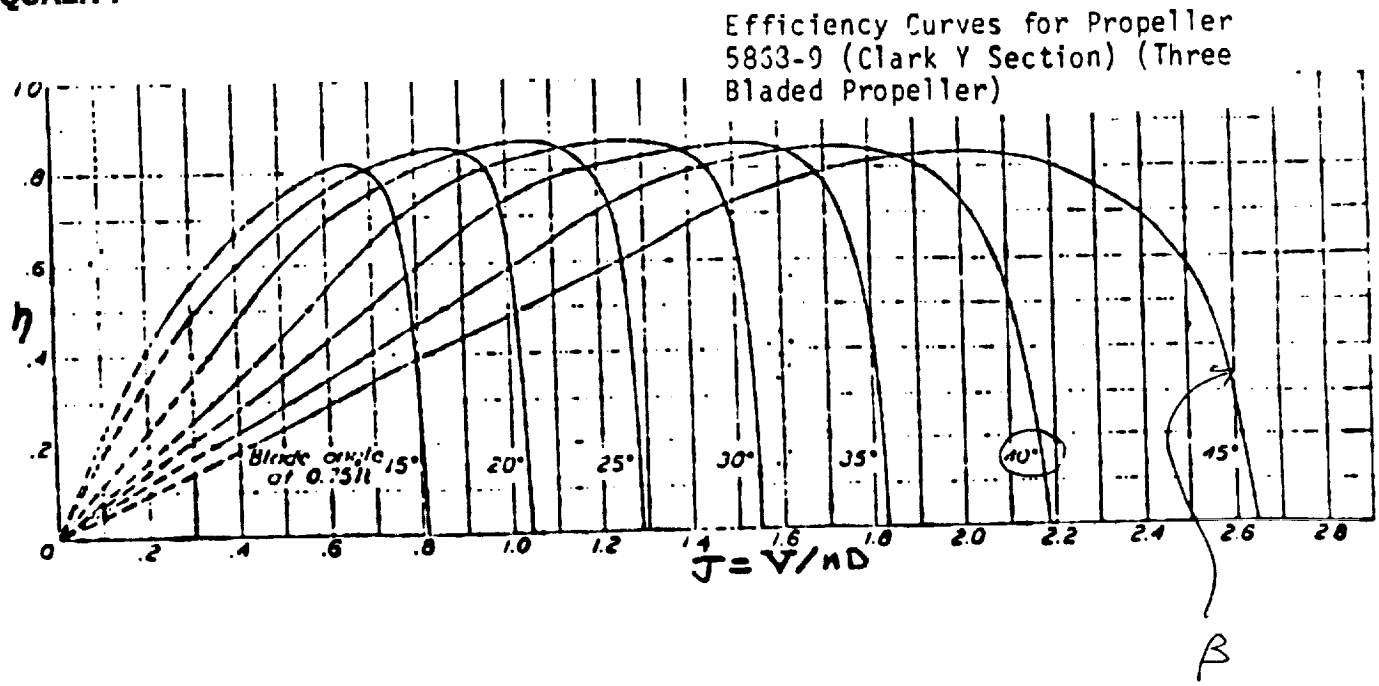

Figure 3-14. Typical Propeller Performance Data Continued.

Source : Atmospheric Flight Mechanics, Nelson and Rimmel

FIGURE 7.1

gives the best efficiency over the range of advance ratios from 0.8 to 2.0. This advance ratio range results from considering propellers of about 2 ft diameter spinning at around 2000 rpm over the flight velocity range 65 to 165 ft/s. Picking the pitch angle proved to be an "eyeballing" process which involves looking at which curve is the "flattest" over the range. Note that this figure is for a Navy 5868-9 three bladed prop using the Clark Y airfoil section. This three bladed data is used to choose appropriate values for MANTA prop design and then an equivalent two bladed prop is found. The Clark Y airfoil section is used because data regarding it is plentiful and research found that propeller performance is a very weak function of the airfoil. Tables 7.1 through 7.4 help to justify the choice of pitch angle by showing that pitch angles of less than 40 degrees are unable to propel the aircraft at higher speeds.

Table 7.1

$V = 65$ ft/s

β (deg)	η (%)
20	30
30	81
35	75
* 40	60

Table 7.2

$V = 95$ ft/s

β (deg)	η (%)
20	0
30	72
35	82
* 40	80

$\beta = 40°$ is best choice for good η over a wide V range.

Table 7.3

$V = 125$ ft/s

β (deg)	η (%)
20	0
30	0
35	0
* 40	77

Table 7.4

$V = 155$ ft/s

β (deg)	η (%)
20	0
30	0
35	0
* 40	0

Next, the diameter of a three bladed propeller is chosen by investigating how props of various diameters behave over the flight velocity range. Figure 7.2 illustrates that for 40 degrees of pitch and a rotational speed of 1800 rpm, a 2.5 ft diameter prop gives the best efficiency over the entire range.

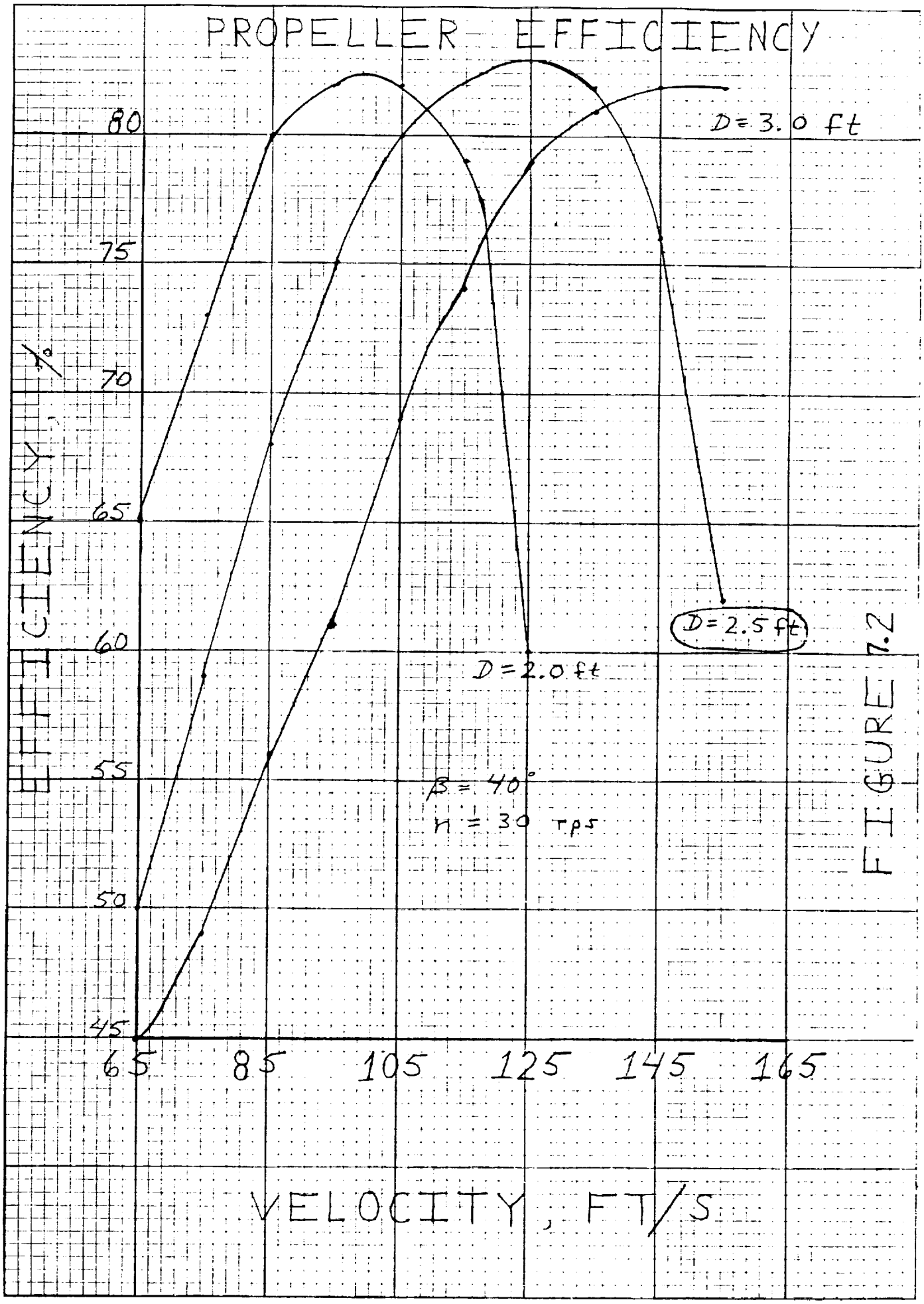

FIGURE 7.2

This three bladed propeller is then turned into an equivalent two bladed screw by keeping the advance ratio constant and finding the rotational speed necessary to get the same efficiency. The designer chooses what diameter he would like for the two bladed prop and keeps the flight velocity constant. This "two bladed equivalence method" works because the advance ratio is nondimensional. This is similar to sizing a wind tunnel model by keeping Reynolds number constant.

Figure 7.3 shows the rotational speed needed for the equivalent two bladed propeller for a diameter range from 1 to 3 ft. The MANTA propeller is two bladed with a diameter of 2 ft and spins at 2400 rpm. This is a reasonable compromise between size and shaft speed and is also well within both constraints.

The maximum speed of the vehicle with this propeller is then checked, and found to be adequate as shown in Figure 7.4.

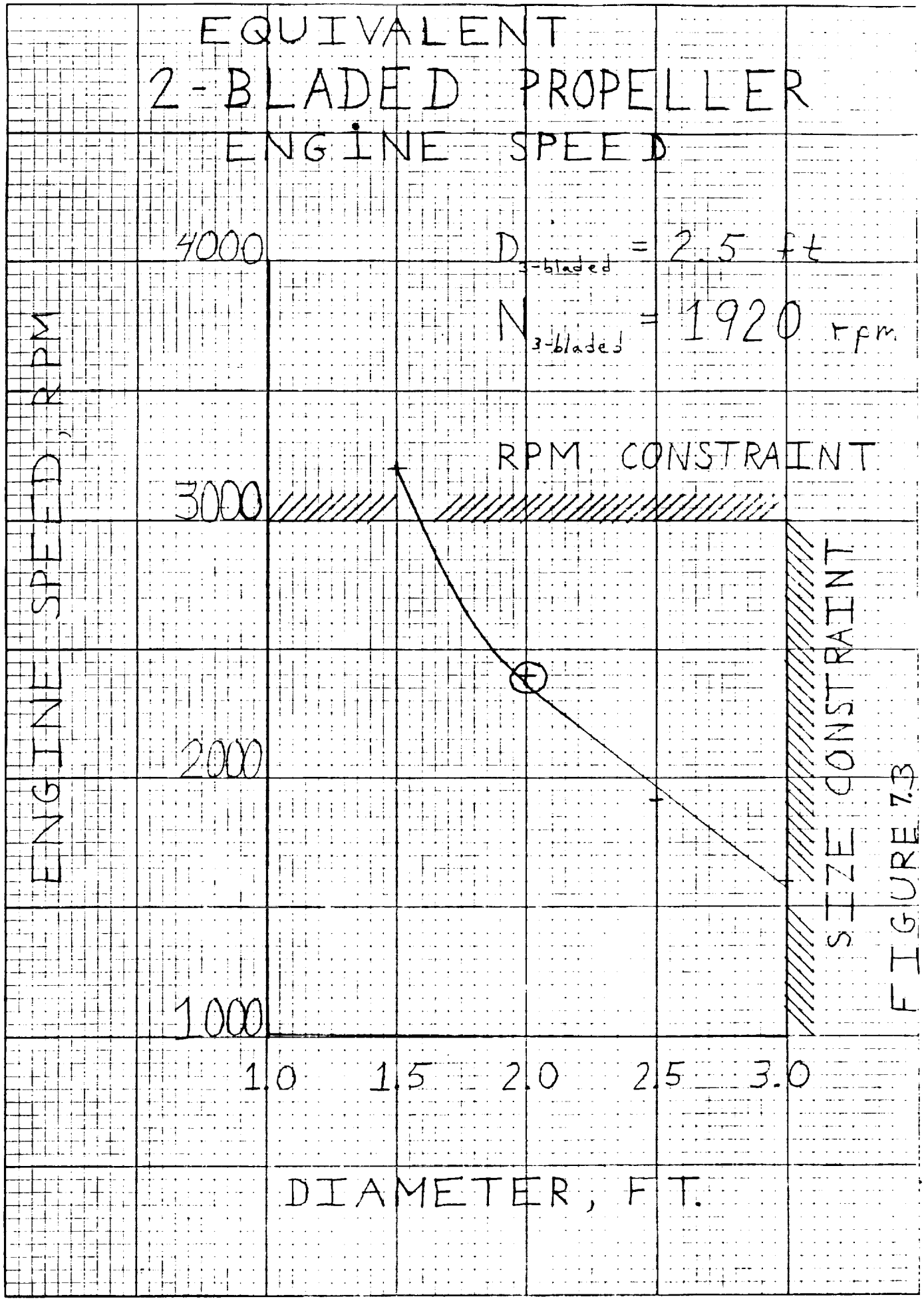

FIGURE 7.3

MAXIMUM VELOCITY FROM PROPELLER

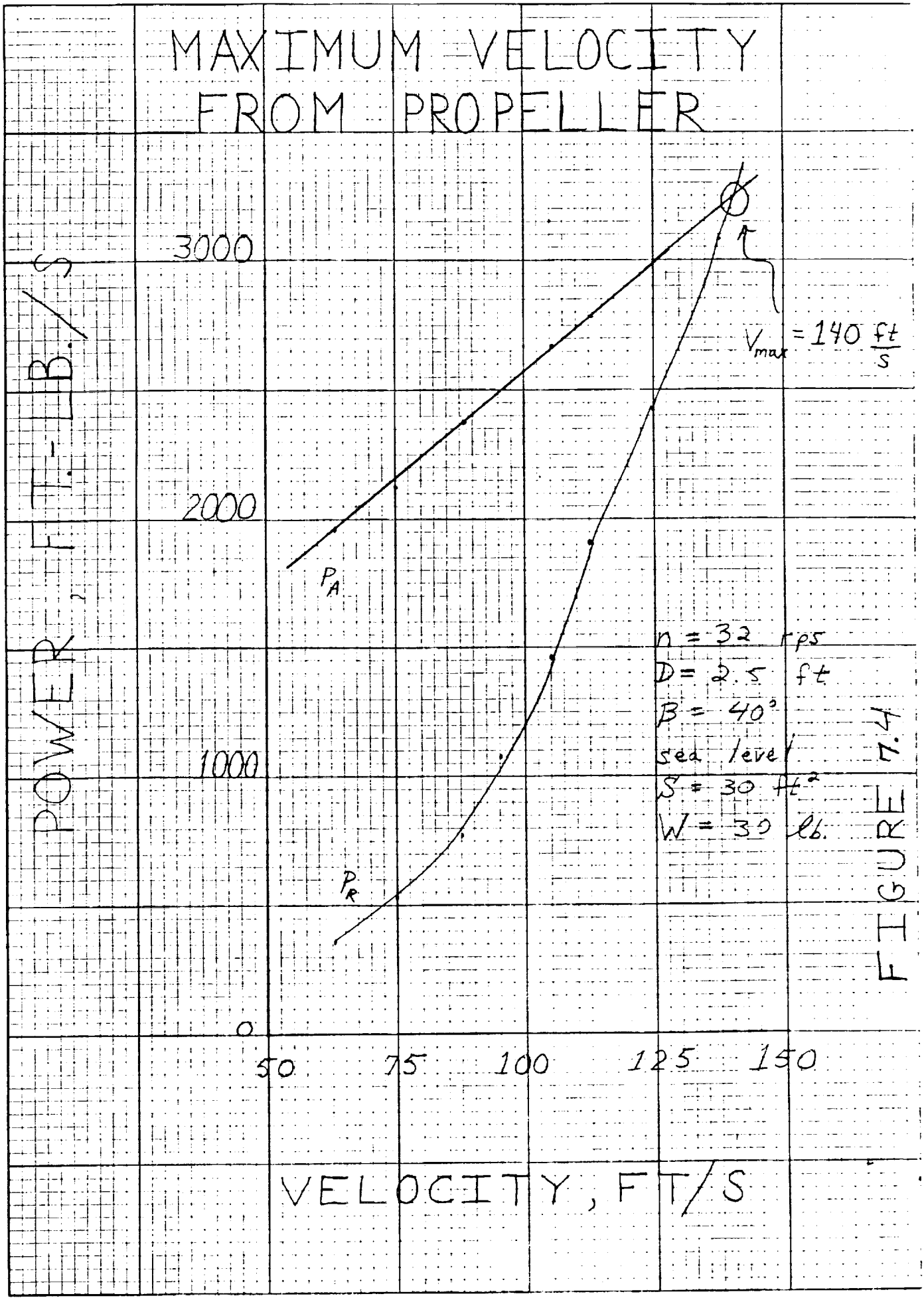

FIGURE 4.4

7.2 Engine Selection

The configuration of the MANTA concept dictates the use of two engines in powering the vehicle to avoid disturbing the airflow along the centerline of the fuselage. This would cause the load data collected on the test specimen to be erroneous. Selection of the engine types to be used involves matching both electric and gas powered reciprocating engines against figures of merit. The engine type which provides best performance for its weight is then selected.

In order to test the upper range of Reynolds numbers, the aircraft must fly at least 140 ft/s. Using the preliminary drag polar

$$C_d = 0.037 + 0.034 * C_l^2$$

the power required for steady level flight at sea level is calculated to be 4.4 bhp. This is the maximum drag condition, and uses the efficiency of the propellers from Figure 7.2. Because the maximum drag condition is being investigated, takeoff requirements can be no worse than those above. Therefore 4.4 bhp is the maximum power output needed from the engines.

A survey of off-the-shelf engines produced several candidates which can satisfy the power requirement. These are preferable to engines designed in-house because of a cost savings. The commercial engines ranged anywhere from 2.0 to 3.0 shaft bhp and each had different fuel consumptions and weights. Figure 7.5 is used to choose the engine based on the weight requirement, while Figure 7.6 minimizes the fuel consumption.

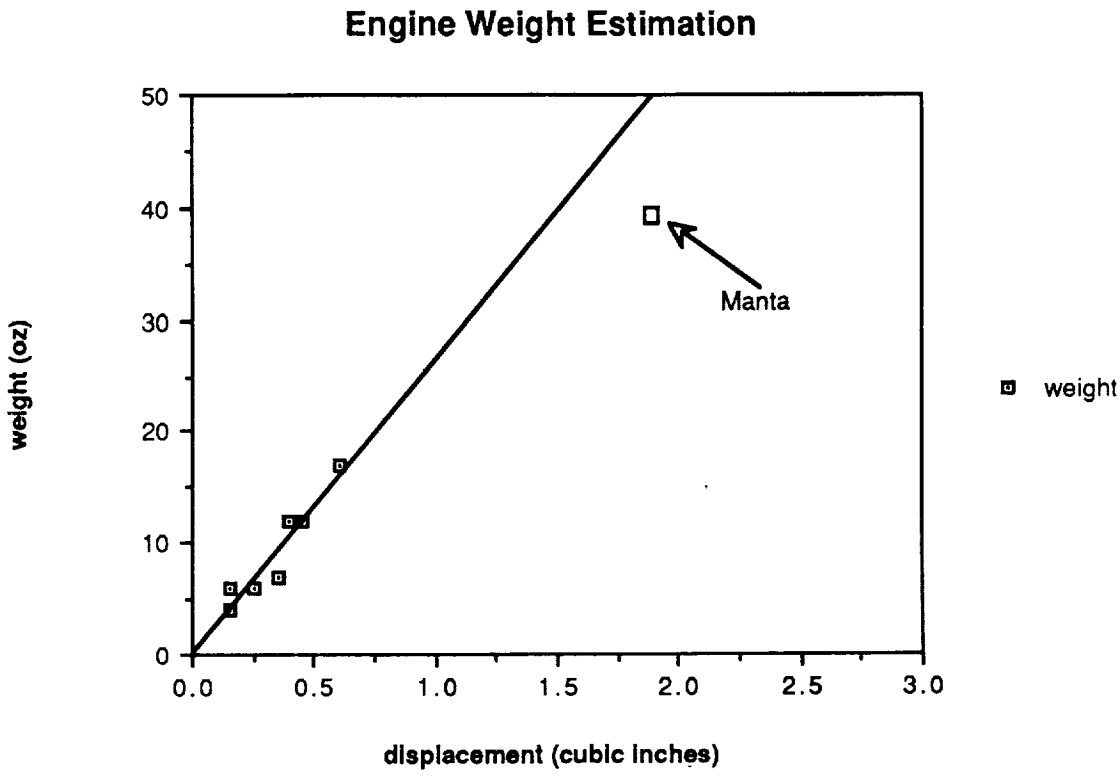
Engine Weight Estimation
50
40
30
20
10
0
weight (oz)
Manta
weight
0.0
0.5
1.0
1.5
2.0
2.5
3.0
displacement (cubic inches)

Figure 7.5

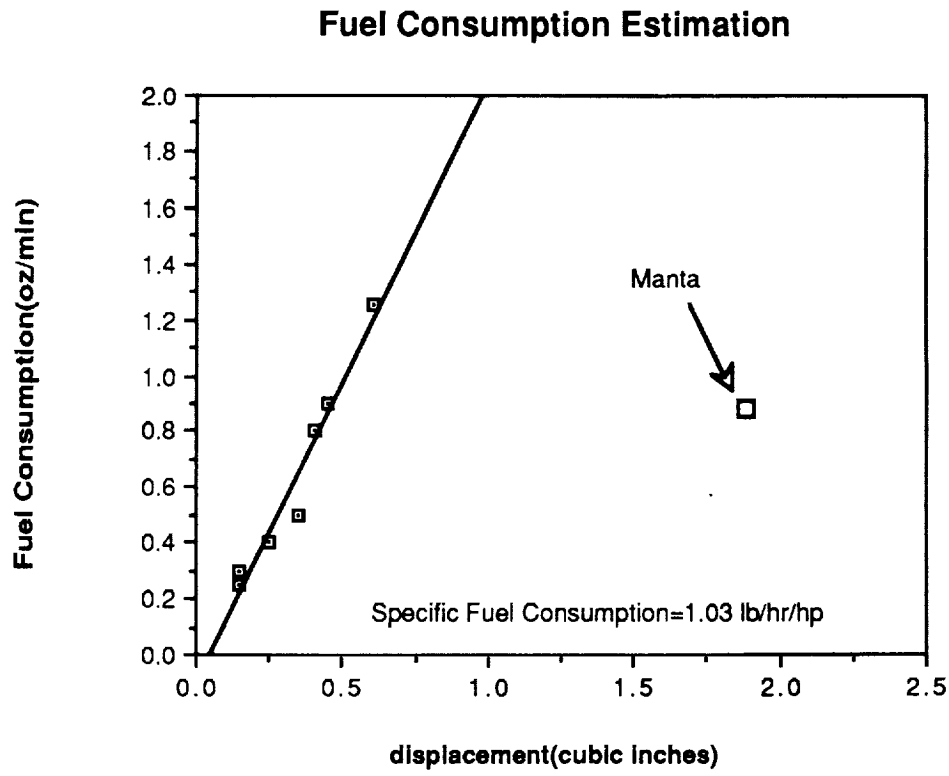
Fuel Consumption Estimation
Fuel Consumption(oz/min)
2.0
1.8
1.6
1.4
1.2
1.0
0.8
0.6
0.4
0.2
0.0
0.0
0.5
1.0
1.5
2.0
2.5
Manta
Specific Fuel Consumption=1.03 lb/hr/hp
displacement(cubic inches)

Figure 7.6

The engine which best meets the design requirements is a 3.0 bhp, 1.82 c.i.d. model power plant. The shaft spins at 7900 rpm and is geared down for the propeller through a 3.3:1 gear ratio. This engine gives the MANTA a total of 6.0 bhp for an available static thrust of 20.8 lb at 115 ft/s. This is the thrust which the propeller must deliver. Figure 7.2, the graph of propeller efficiency, shows that the prop efficiency remains fairly constant between an advance ratio of 1.4 and 1.9. The maximum velocity of the aircraft with both engines at full throttle is 140 ft/s. This barely meets the Reynolds number requirement and in actual operation, the upper Reynolds numbers may be unattainable on the test specimen.

If off-the-shelf engines were not available, an engine could have been designed by calculating the work and displacement of each cylinder. Knowing the displacement, one may then choose the stroke length or bore of the cylinder. Choosing one sets the other. This was not necessary in MANTA's case because sufficient support was available on the commercial market.

Estimation of specific fuel consumtion and total engine weight proved to be very challenging. Manufacturer specifications listed neither, since the market for these engines was the hobby airplane modeler. A data base was used to estimate these quantities as shown in Figures 7.5 and 7.6. One problem with the data base, however, was that no information existed on the fuel consumption and weight of larger displacement engines. To fill this data gap, tests were run on a lawnmower, chainsaw, and snowblower. The chainsaw had a similar engine size to that used in many model aircraft. The tank was filled with a known amount of fuel, run for a certain length of time, and the remaining fuel was measured. In this manner, the specific fuel consumption was calculated. Plotting this fuel consumption with the other data, it becomes obvious that no simple relationship exists to predict the fuel consumption from the database. Therefore, the chainsaw data was taken as the most relevant and used for the MANTA's calculations.

Engine weight was estimated by using rules of thumb. The actual cylinder of the engine accounts for about one third of the total engine weight. Increasing the displacement of a smaller engine would then result in doubling its weight. Adding about 20% more due to the increase in the base area established an engine weight of approximately 2.5 lb per engine. It is important to note that this is a rough estimate based on the assumption that a 20% bigger base is needed to support a bigger

cylinder.

The final important selection for the MANTA's engines was the fuel type to be used. The fuel for model aircraft consists of a mixture of castor oil, methanol, and nitromethane. The amount of nitromethane in the fuel determines the performance of the engine. Too much nitromethane, usually on the order of 35% in the mixture, will not stay mixed in the fuel. If no nitromethane is used, then the fuel will not burn as hotly, reducing power output and efficiency of the combustion process. This leads to a premature buildup of thickened oil, called varnish, which reduces engine performance and life. For the MANTA, a fuel mixture of 10% nitromethane, 20% methanol, and 70% castor oil is used. This allows the nitromethane to stay mixed, but still allows combustion to occur at high temperature for good thermal efficiency.

7.3 Conclusion

The propulsion system of the MANTA flight vehicle is designed for the following considerations:

a) Enabling tests at Reynolds numbers of 1 million on the test specimen.

b) Providing adequate power for steady level flight and an adequate maximum speed to meet the requirement above.

The system chosen to meet the requirements has two reciprocating internal combustion engines utilizing propellers specifically designed for the MANTA's wide flight velocity range. The upper Reynolds number range may be unattainable in reality, although calculations show that MANTA should just barely be able to attain the speed necessary. The system does indeed provide adequate power for steady, level flight and takeoff performance is not a problem.

8.0 TAKEOFF PERFORMANCE

8.1 CONVENTIONAL GROUND ROLL TAKEOFF

The MANTA is not able to accomplish any of its data acquisition if it is unable to get into the air. Early on in the design stage many launching techniques were investigated. Some of these were a high start technique, a catapult launch, and a drop from a carrier aircraft; along with the conventional ground roll takeoff. The high start and catapult launch techniques were disregarded for two reasons. The first concern was the rapid acceleration seen in both cases. This causes problems with the delicate instrumentation that is aboard the MANTA, along with placing increased stresses on the structure of the MANTA. A second reason these techniques were disregarded is the desire to keep the MANTA as simple to operate as possible. Of the four types of takeoffs, these caused the most difficulties and problems.

The drop from a carrier ship eliminated any difficulty of getting the MANTA into the air. However the cost of the project would increase dramatically by bringing a full scale aircraft into the experiment. Also the difficulty of operation increased due to the increase in the number of people needed to run the testing.

The MANTA takes off from a conventional ground roll. This is the most familiar takeoff known to RPVs and RPV pilots. The only additional cost added to the MANTA for this type of takeoff was the landing gear.

8.2 TAKEOFF REQUIREMENTS AND CONSIDERATIONS

The MANTA is required to takeoff in a circular area with a radius of 150 ft and an object clearance of 50 ft. In order to determine the MANTA's capabilities to meet these requirements, a parametric trade study was done varying the horsepower, density, weight, and propeller efficiency.

The MANTA's horsepower capability is near 4.8 hp with its twin engine configuration. Most of the study was done at values much less than this. However there are a number of noticeable trends that exist in the data base that determine the MANTA's ability to takeoff. For the propeller efficiency (approximately 0.4-0.8 for the MANTA) there is basically little effect on the ground roll distance. The type of propeller chosen is not a significant concern for takeoff (see Figure 8.1).

FIGURE 8.1 PROP EFFICIENCY EFFECT ON TAKEOFF

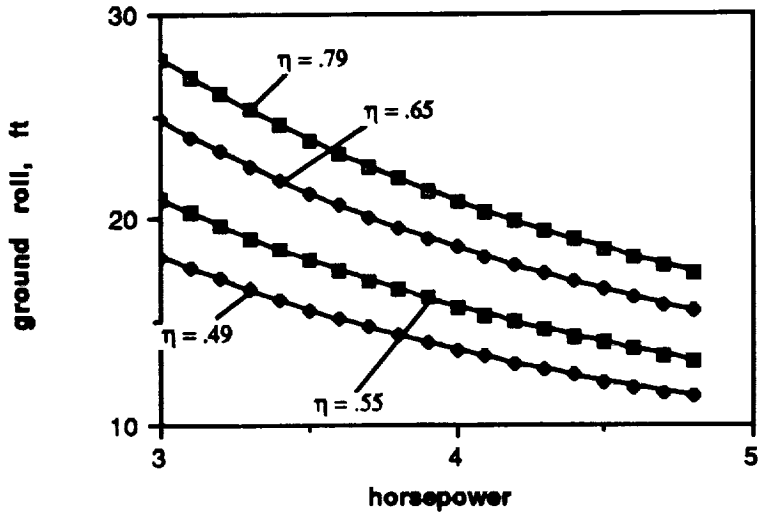

Figure 8.1

As for the weight of the MANTA, of course the lighter the vehicle remained, the shorter the ground roll distance. At weights above the 30 lb category, the effect horsepower had on takeoff started to become significant. In order to obtain a ground roll distance within the requirements, the MANTA's weight is to be kept near the 30 lb class (see Figure 8.2).

FIGURE 8.2 WEIGHT EFFECT ON TAKEOFF

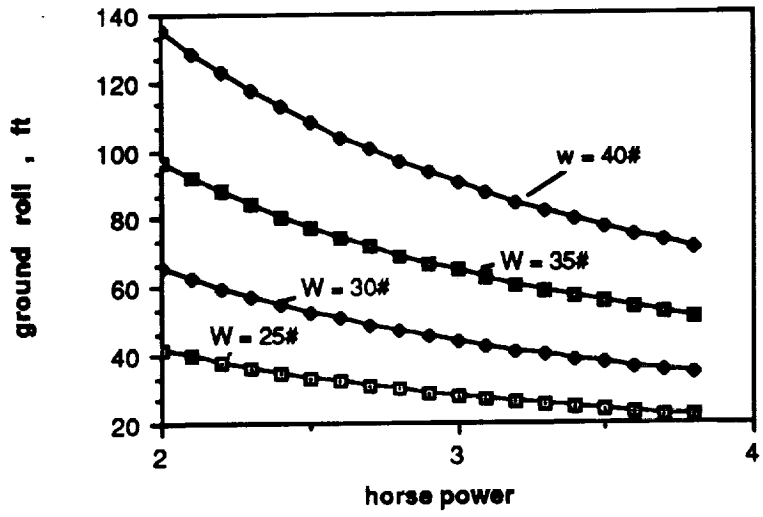

Figure 8.2

FIGURE 8.3 DENSITY EFFECT ON TAKEOFF

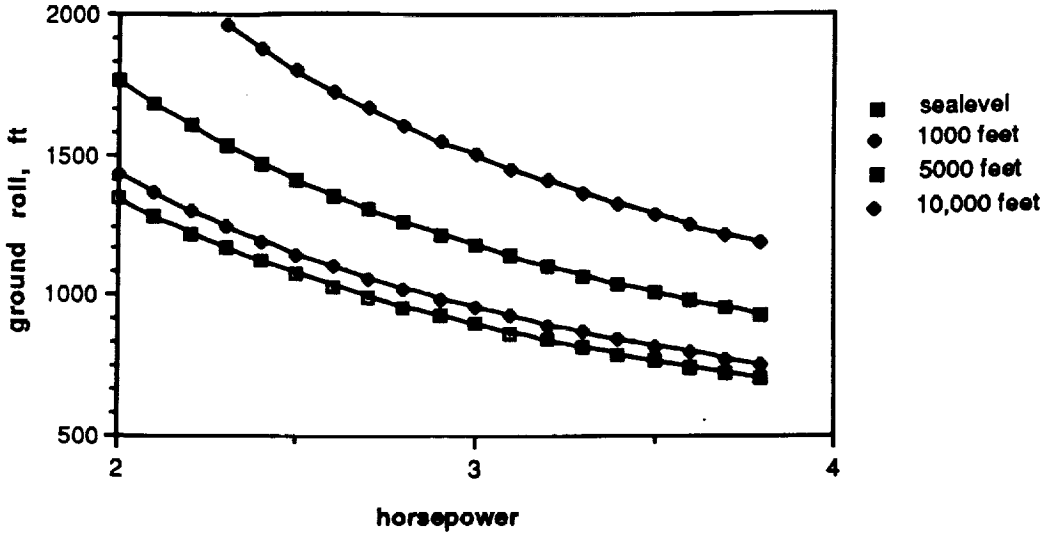

The Cl and density effects on the ground roll of the MANTA can both be controlled relatively easy. To optimize the Cl, it is imperative to mount the landing gear such that the wing isat an angle of attack just below the maximum Cl of the wing. The density can be controlled by placing an altitude ceiling for takeoff (see Figures 8.3 and 8.4).

FIGURE 8.4 Cl EFFECT ON TAKEOFF

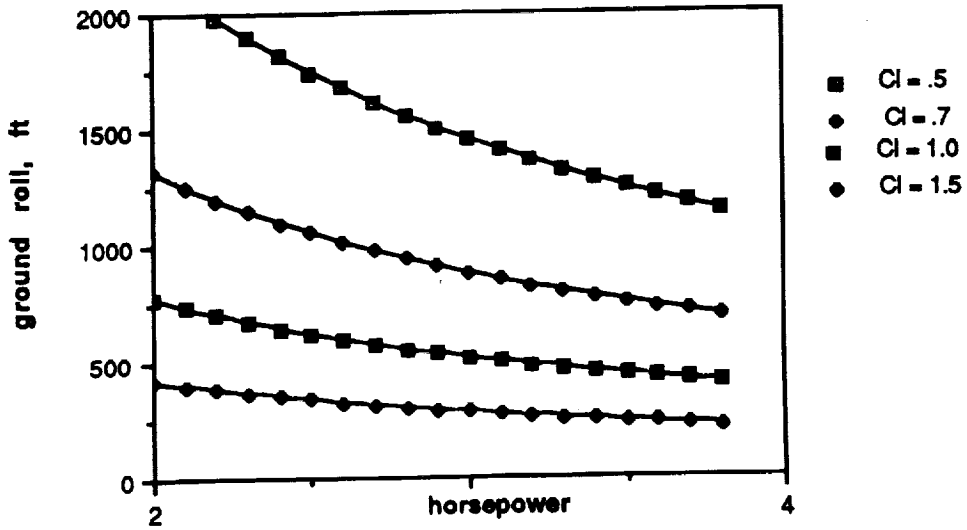

8.3 TAKEOFF CHARACTERISTICS AND RECOMMENDATIONS

After analyzing the data, it was decided the horsepower of the MANTA's propulsion systems needed to be near 4.5 hp. As it stands, the MANTA's engines produce 4.8 hp of usable power from the propellers. The weight of the MANTA also is near the recommended 30 lb class, actually weighing 32 lbs.

For the takeoff of the MANTA it is recommended that the surface be relatively flat and smooth. A concrete or asphalt runway is sufficient. The MANTA is capable of taking off in a grassy field, however it may not be capable of meeting the 150 ft radial takeoff requirement. Also the requirement can not be met at an altitude above 1000 ft and seems impossible to takeoff above an altitude of 5000 ft where the ground roll distance becomes far too large at the horsepower available.

The MANTA's landing gear is mounted such that the wing is at an angle of attack of 11 degrees to optimize the lift of the wing during ground roll and takeoff. This provides a Cl of about 1.2, sufficient for a 300 ft ground roll with the MANTA's horsepower. At sea level with a full payload and fuel the MANTA is capable of taking of with a ground roll near 200 ft.

9.0 PRODUCTION AND MANUFACTURING

Most of the MANTA is made of spruce, balsa, and basswood. Because of the simplicity of production materials the MANTA can be built in-shop. In order to ensure the accuracy of certain parts, the producers recommend that some of the manufacturing and production be contracted out to professionals. Two examples of possible contracting lay in the making of the wing and the building of the force balance system. Having a professional wood cutter manufacture the wings will help to reduce the material error in the reproduction of ribs and spars which the wing needs in order to maintain its best possible efficiency. Secondly, a professional measurements company should install the strain guages needed for the force balance system. Professional installation will improve accuracy in data collection and reduce production time, however, an increase in cost will occur. Because the accuracy of data remains the most important priority of the MANTA project, the extra installation cost can easily be justified.

There are six main components in the production of the MANTA. The first two are relatively obvious, the wing and the fuselage. Two other major parts include the control surfaces and the internal payload packages. A fifth component of the flight vehicle is the propulsion system. As stated before, the wings will be contracted out to professionals. Aside from the wood cutter, a second part of the contract would also include the installation of the necessary fuel lines, servos, and speed controller for the engines. The manufacturer of the wing will also manufacture the nacelles and return the two parts to the original designers who can integrate the two in conjunction with the engine to ensure that the propulsion system works well. The sixth part, and key to the integration

of all these components of the aircraft, as well as to its success, becomes the data acquisition package including, transducers, amplifiers, filters, multiplexer, A/D converter, memory storage chips, the receiver, and the transmitter. The placement of each part of the internal payload system becomes the important key to proper operation of the MANTA and its major goal of accurate data acquisition. Although it might seem appropriate to also contract out this part of production, we feel that the construction group itself should perform the installation of the internal payload in order that it can troubleshoot the system should problems arise.

As stated before, the simplicity of the construction materials of the MANTA make it simple to purchase and build. Although some professional contracting will help to improve the quality of the vehicle, most of the plane will be manufactured in-house. In-house installation of the most complex system (the data acquisition system) will insure that problems which arise during the production phase of the project will be taken care of by the initial designers of the vehicle.

10.0 Cost Analysis

Although the design group did not consider cost as a primary priority in the initial planning of the MANTA RPV aircraft, one obviously realizes that an accurate cost analysis of the aircraft is required in order to justify the proposed design. The cost analysis of the MANTA is broken into four parts. The parts of the analysis, each representing a specific system of the plane are as follows: Control system cost, Propulsion system cost, Instrumentation/Data Acquisition System cost, and Construction materials cost.

The cost of the control system is broken up into three parts labelled as heavy-duty servos, push rods, and control devices. The cost of the control system comes to $301.00, approximately 5.1% of the total flight vehicle cost.

The cost of the propulsion system is broken up into two parts. The first part considers the cost of two gas powered, propeller driven engines. The second part considers the cost of fuel, fuel tanks, and fuel lines for the aforementioned engines. The total cost of the propulsion system comes to $600.00, approximately 10.2% of the flight vehicle cost.

The cost of the instrumentation/data acquisition system (DAS) is the most complicated to figure. The first priority of the MANTA is for it to collect reliable data over a large test range, therefore, the instrumentation group needed to find very high quality instruments to complete its system. However, the issue of cost was always considered so that the flight vehicle could provide an outstanding, yet cost-efficient data acquisition system. The DAS was composed of three major subgroups. The first part consisted of strain gages and transducers, both of which were used in the actual data collection and transformation. The second part consisted of the computer, used as a ground based autopilot for the airplane and its related components. The final part of the

system consisted of the batteries used to power the DAS. The total cost of the DAS came to $4,540.00, approximately 77.4% of the total flight vehicle cost.

The cost of flight vehicle construction was broken up into cost for wood and the cost of miscellaneous supplies. The cost of vehicle construction came to $325.00, approximately 5.3% of total flight vehicle cost.

The MANTA flight craft will have a production cost of $5,866 (not including designing, labor, maintenance, etc.). Fig. 10.1 provides a detailed cost breakdown for the entire flight vehicle by system.

Figure 10.1 Cost Breakdown

System	Cost
1. Control System	
a. Heavy Duty Servo (4 @ 60)	240.00
b. Push Rods	
1. Empenage (2 @ 8)	16.00
2. Other (3 @ 5)	15.00
c. Control Devices (15 @ 2)	30.00
	$ 301.00
2. Propulsion System	
a. Engines	400.00
b. Fuel/Tanks/Fuel Lines	200.00
	$ 600.00
3. Instrumentation/Data Acquisition System	
a. Batteries	25.00
b. Strain Guages	25.00
c. Transmitter/Receivers	600.00
d. A/D Converter	500.00
e. Onboard Memory Storage Chips	500.00
f. Transducers	500.00
g. Encoders/Filters	390.00
h. Autopilot (computer)	2000.00
	$ 4540.00
4. Construction Materials	
a. Balsa/Spruce Wood	250.00
b. Miscellaneous Supplies	75.00
	$ 325.00
Total Cost	**$5866.00**

11.0 ENVIRONMENTAL CONCERNS

In sizing up the possible environmental concerns, it is helpful to note that the rules of common sense apply. The MANTA should provide similar environmental concerns to those of a "sport" RPV. Three areas are of concern--noise, impact from a crash, and fire.

Being gas powered, the MANTA's engines will produce more noise than an electrically powered RPV. However, from experience with previous gas powered RPVs, this noise should not be excessive, certainly not to an environmentally-threatening level.

A somewhat greater concern would be damage to the environment caused by a crash or mid-air breakup resulting from a catastrophic failure of the vehicle. This would be a concern from a safety standpoint. The operational area should preferably be free of unnecessary persons, or a large amount of wildlife.

Of greatest environmental concern would be fire. Care must be taken during the refueling phase of the mission. Also, though the amount of fuel carried on-board the vehicle is small, this could be enough to start a major fire. Three precautions are merited. First, no flights should be undertaken if the operational area is extremely dry and has been for a long period of time, such as in a draught. Second, a fuel cutoff valve should be installed which would shut off fuel flow from the tanks if the shaft stops rotating. This would help in the case where the fuel line is severed, but the tank is still intact. Finally, the fuel-carrying sections in the wings should be sealed to prevent leakage.

12.0 MANTA Technology Demonstrator

12.1 The MANTA technology demonstrator was built to test the flight worthiness of the longitudinal stability system. It was this system that was of the greatest concern when the design originated, and it was therefore the main thrust behind our technology demonstration. In addition to this, it was desired to retain most, if not all, of the MANTA's physical characteristics. This includes the twin-boom data acquisition structure and the overall structural make-up of the wings and fuselage.

12.2 The design of the technology demonstrator was a half scale of the original design concept. In reducing the dimensions of the MANTA, all elements were built exactly like they were designed for the original concept. The technology demonstrator was constructed mainly from balsa, spruce, and plywood. The entire structure was covered with a plastic monocoat.

Due to the fact that the technology demonstrator retained the twin-boom structure, it was not possible to mount a single engine on the fuselage nose. It was also not possible to place it above the fuselage as it would adversely affect the longitudinal stability of the aircraft. Therefore, a dual engine propulsion system was required. Gas engines were chosen for the demonstrator due to weight control considerations and wing-mounting problems.

The technology demonstrator successfully flew on 27 April 1989, demonstrating its flight worthiness. The aircraft stayed in the air for approximately 50 seconds, at which point the vertical stabilizer snapped off. In an attempt to retain stability, the pilot throttled back on the power causing one of the engines to stall. This resulted in a spin taking the aircraft into the ground. There was little aircraft remaining.

Although the test flight time was limited, several observations were made. First, the test of the longitudinal stability system was successful as the aircraft trimmed and

handled well. There was some concern about flutter in the longitudinal and lateral control systems which occured during the flight. However, this was attributed to play within the surfaces rather than any inherent design fault.

Wing warping during the flight test was a further observation. This may represent a need for added structural support in the design. Aside from these problems, the flight did demonstrate that the MANTA design can achieve effective turn and climb rates. After the short takeoff and vertical landing demonstration of the MANTA aircraft, there can be no doubt that the MANTA will be the most talked about RPV at Notre Dame for years to come.